Cell Metabolism

Article

Gut microbiota regulates stress responsivity via the circadian system

Graphical abstract

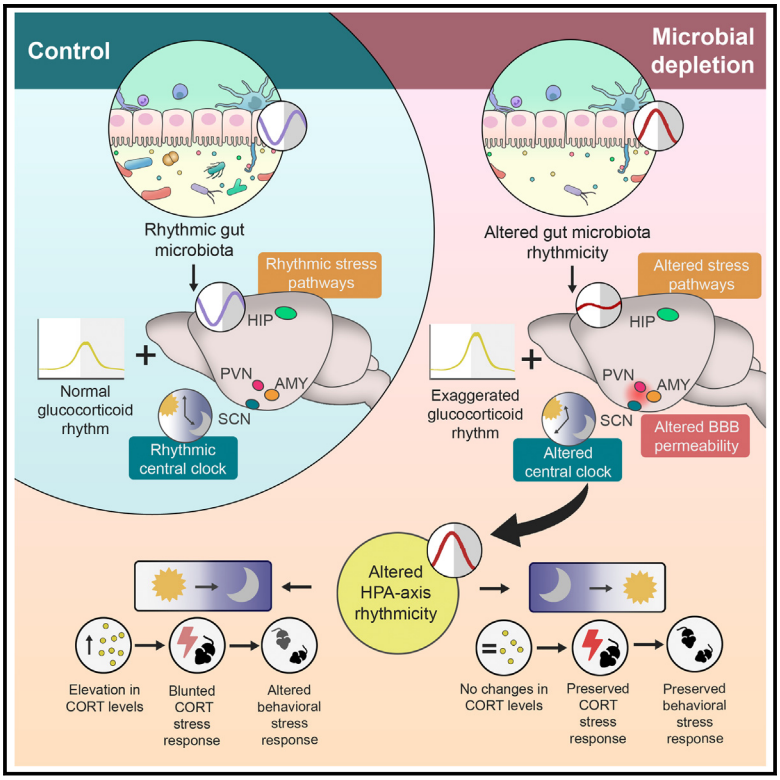

Highlights

- Gut microbiota regulates diurnal rhythms of corticosterone
- Microbial depletion leads to disruption in rhythmicity of stress pathways in the brain
- Microbial depletion results in time-of-day-specific impairments in stress responsivity
- Diurnal oscillations of gut microbes modulate corticosterone release

Authors

Gabriel S.S. Tofani, Sarah-Jane Leigh, Cassandra E. Gheorghe, ..., Paromita Sen, Gerard Clarke, John F. Cryan

Correspondence

j.cryan@ucc.ie

In brief

Gut microbes are known to modulate stress responsivity and behavior. Tofani et al. demonstrate that such modulations occur via the circadian system. The oscillations in gut microbiota composition regulate the diurnal rhythmicity of hypothalamic-pituitary-adrenal (HPA)-axis function, which leads to altered stress responsivity across the day.

Tofani et al., 2025, Cell Metabolism *37*, 1–16
January 7, 2025
https://doi.org/10.1016/j.cmet.2024.10.003

CellPress

Cell Metabolism

CellPress
OPEN ACCESS

Article

Gut microbiota regulates stress responsivity via the circadian system

Gabriel S.S. Tofani,[1,2] Sarah-Jane Leigh,[1,3] Cassandra E. Gheorghe,[1,3] Thomaz F.S. Bastiaanssen,[1,2] Lars Wilmes,[1,2,3] Paromita Sen,[1,2] Gerard Clarke,[1,3] and John F. Cryan[1,2,4,*]

[1]APC Microbiome Ireland, University College Cork, Cork, Ireland
[2]Department of Anatomy & Neuroscience, University College Cork, Cork, Ireland
[3]Department of Psychiatry & Neurobehavioral Sciences, University College Cork, Cork, Ireland
[4]Lead contact
*Correspondence: j.cryan@ucc.ie
https://doi.org/10.1016/j.cmet.2024.10.003

SUMMARY

Stress and circadian systems are interconnected through the hypothalamic-pituitary-adrenal (HPA) axis to maintain responses to external stimuli. Yet, the mechanisms of how such signals are orchestrated remain unknown. Here, we uncover the gut microbiota as a regulator of HPA-axis rhythmicity. Microbial depletion disturbs the brain transcriptome and metabolome in stress-responding pathways in the hippocampus and amygdala across the day. This is coupled with a dysregulation of the circadian pacemaker in the brain that results in perturbed glucocorticoid rhythmicity. The resulting hyper-activation of the HPA axis at the sleep/wake transition drives time-of-day-specific impairments of the stress response and stress-sensitive behaviors. Finally, microbiota transplantation confirmed that diurnal oscillations of gut microbes underlie altered glucocorticoid secretion and that *L. reuteri* is a candidate strain for such effects. Our data offer compelling evidence that the microbiota regulates stress responsiveness in a circadian manner and is necessary to respond adaptively to stressors throughout the day.

INTRODUCTION

The stress and circadian systems are intertwined, being an evolutionary conserved adaptation that allows the organism to respond to changes in the environment.[1] Although the stress response is characterized as a rapid adaptive process to actual or perceived danger,[2] the circadian rhythm is an endogenous process that anticipates predictable environmental cues.[3] Although these two systems have different functions, their overlapping nature is clear because the main pathways that distribute circadian and stress-related information are the same: the hypothalamic-pituitary-adrenal (HPA) axis and the autonomic nervous system.[4] Moreover, the suprachiasmatic nucleus (SCN), the central circadian pacemaker, and the paraventricular nucleus (PVN) of the hypothalamus, the main driver of the stress response in the brain, are close in proximity and interconnected.[5]

Glucocorticoids produced following activation of the HPA axis are a core component of both circadian and stress systems.[6] Besides being a main effector of the stress response,[7] glucocorticoids display a peak at the sleep/wake transition that functions as one of the main synchronizing circadian cues from the brain to the periphery.[8,9] This rhythmic pattern of glucocorticoids is maintained by the SCN.[10] Due to this oscillating nature, the magnitude of this stress-driven glucocorticoid increase is lower when the stressor is performed at the circadian peak compared with the circadian trough.[11–13] Additionally, alterations to the rhythmicity of glucocorticoids have been associated with an impaired stress response.[14] Although it has been known since the 1970s that time of day can impact the glucocorticoid stress response, the mechanisms underlying how the organism integrates circadian and stress inputs to maintain appropriate stress responsiveness are still unresolved.

In addition to playing a central role in both stress and circadian signaling, the HPA axis has also been shown to be one of the key pathways through which the gut microbiota can shape brain function and behavior.[15] The trillions of microorganisms that reside in the gut have co-evolved with their hosts, resulting in an intertwined relationship between the gut microbiota and host physiology.[16] In particular, the hippocampus and amygdala have been shown to be sensitive to gut microbial modulations.[17] Stress-induced glucocorticoid release has been demonstrated to be modulated by the gut microbiota because germ-free (GF) mice display exaggerated glucocorticoid levels following stress that can be recovered upon colonization.[18,19] Additionally, the gut microbiota displays strong diurnal oscillations in composition and metabolic output that are important to maintain metabolic health,[20–25] and microbial depletion has been demonstrated to lead to altered baseline levels of glucocorticoids at different times of the day.[26] Further indication of the importance of the crosstalk between stress, circadian rhythms, and the microbiota emerges from a growing literature on stress-related psychiatric disorders that often display disruption in clock-regulated

Please cite this article in press as: Tofani et al., Gut microbiota regulates stress responsivity via the circadian system, Cell Metabolism (2024), https://doi.org/10.1016/j.cmet.2024.10.003

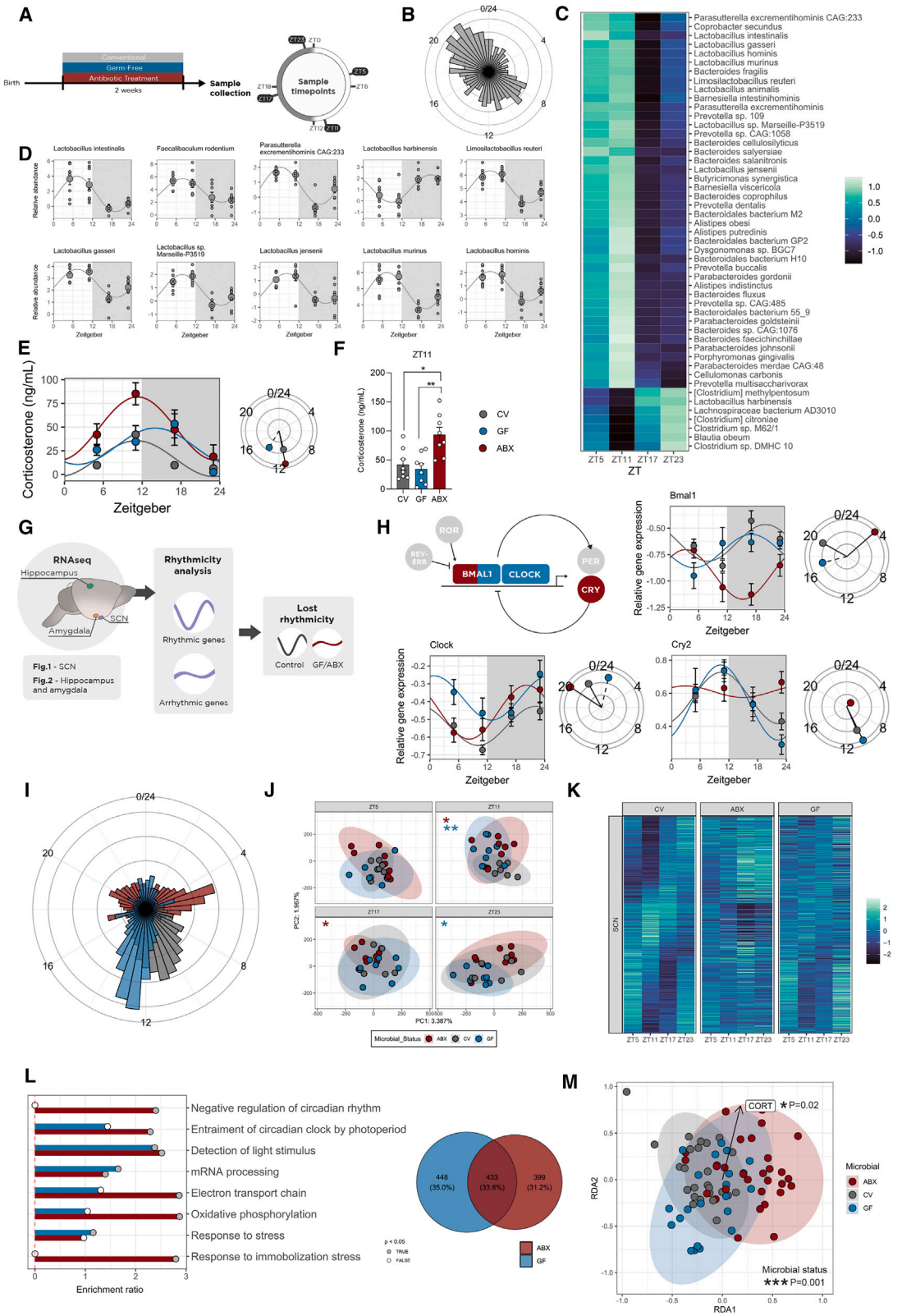

(legend on next page)

Please cite this article in press as: Tofani et al., Gut microbiota regulates stress responsivity via the circadian system, Cell Metabolism (2024), https://doi.org/10.1016/j.cmet.2024.10.003

processes and microbiota composition.[27–29] The current literature indicates evidence that gut microbes regulate brain function, the stress response, and circadian rhythms, but such studies were conducted independently, with the integrative aspect of such modulation remaining completely unknown.

To this end, we investigate the circadian-stress interplay in the absence of gut microbiota to understand how gut microbes can shape the interactions between the stress and circadian systems. First, we establish that the gut microbiota regulates the diurnal rhythms in glucocorticoids, what is linked with alterations in circadian rhythmicity in the SCN transcriptome. Next, by investigating the alterations in rhythmicity induced by the gut microbiota in the transcriptome and metabolome of the hippocampus and amygdala, we show a disruption in pathways key to maintaining appropriate stress responsiveness. Furthermore, we explore how these changes in rhythmic glucocorticoids are driven, demonstrating a hyper-activation of the HPA axis following microbial depletion, which drives time-of-day effects on the stress response and behavior. Lastly, we investigate the compositional changes in the microbiota underlying the alterations in glucocorticoids to show that diurnal oscillations in gut microbes drive such changes. Thus, together this work identifies the gut microbiota as an important orchestrator of the interactions between the stress and circadian systems.

RESULTS

Gut microbiota oscillates across the day and modulates diurnal rhythms of corticosterone

The gut microbiota display diurnal oscillations that are key to maintain host metabolic health,[20,22–25] but the impact of such oscillations in brain function remains unexplored. To address this question, we used metagenomic sequencing to determine oscillating patterns of the microbiota from control animals at the strain level (Figure 1A). In accordance with previous reports, we show that gut microbes oscillate across the day (Figures 1B and 1C). Such diurnal variation was especially significant for the genus Lactobacillus, which comprised seven out of the 10 strains with the highest amplitude in the mice gut (Figure 1D). Interestingly, among those bacteria, were species commonly used as probiotics, such as *Limosilactobacillus reuteri* (formerly known as *Lactobacillus reuteri*) and *Lactobacillus jensenii*.

HPA-axis stress-responding and baseline corticosterone levels are known to be modulated by the gut microbiota.[18,19,30,31] Because we observed changes in the composition of the gut microbiota across the day, we aimed to assess whether the influence of the gut microbiota on HPA-axis function is time-of-day dependent. To this end, we collected samples across the day in animals with a microbiota depleted by antibiotic treatment (ABX) or GF status (Figure 1A). Here, we discover that the diurnal rhythm of plasma corticosterone is disrupted by microbial status. More specifically, the sleep/wake peak that is characteristic of this hormone is shifted to the dark phase in GF mice, whereas ABX mice display an increase at zeitgeber time (ZT) 11, which resulted in a higher rhythm amplitude (Figures 1E and 1F). Alongside glucocorticoids, catecholamines are also central to the stress response.[32] Although no changes in diurnal plasma noradrenaline levels were observed (Figure S1A), adrenaline in ABX mice displayed differential rhythmicity compared with conventional (CV) mice, with a higher amplitude similar to that of corticosterone (Figure S1B).

Absence of gut microbiota alters master clock rhythmicity

Because glucocorticoids serve as a major circadian and stress signal,[6] we sought to understand if these microbiota-driven disruptions of rhythm also manifest in regions of the brain involved in the integration of stress and circadian signals. We performed RNA sequencing of the SCN, hippocampus, and amygdala because such regions are important for both circadian and stress regulation. We first assessed rhythmicity of the

Figure 1. Gut microbiota oscillates across the day and modulates rhythmicity of corticosterone and the SCN transcriptome

(A) Experimental design schematic.

(B) Acrophase plot of all transcripts after rhythmicity analysis (n = 6–8/group/time point) (bars represent the number of genes exhibiting their acrophase at each time point). Rhythmicity analysis was conducted by linear modeling to a Fourier-decomposed sine and cosine element for circadian rhythmicity followed by Tukey-adjusted post-hoc comparisons.

(C) Heatmap displaying the top 50 oscillating bacterial strains in the mouse gut with the highest amplitude. Values are displayed as group average.

(D) Top 10 oscillating bacterial strains in the mouse gut by highest amplitude. Line plot shows the real (dot and error bar represent mean ± SEM) and predicted (line) relative abundance.

(E) Circulating levels of corticosterone across the day (n = 4–8/group/time point). Line plot shows the real (dot and error bar represent mean ± SEM) and predicted (line) corticosterone levels, whereas circle plots show the predicted acrophase for each group (solid line: $p < 0.05$, dashed line: $p > 0.05$).

(F) Corticosterone levels at ZT11. Data analyzed using one-way ANOVA followed by Tukey-adjusted post-hoc comparisons.

(G) Rhythmicity analysis schematic.

(H) Schematic representing transcriptional-translational feedback loop of core clock genes and proteins and respective altered transcripts in the suprachiasmatic nucleus (SCN), colors in the schematic indicate genes statistically altered in ABX (red) and GF (blue) mice. Line plots show the real (dot and error bar represent mean ± SEM) and predicted (line) gene expression for key clock genes in the SCN, whereas circle plots show the predicted acrophase for each group (solid line: $p < 0.05$, dashed line: $p > 0.05$).

(I) Acrophase plot of all transcripts after rhythmicity analysis (n = 7–8/group/time point) (bars represent the number of genes exhibiting their acrophase at each time point).

(J) Principal component analysis of the SCN transcriptome in each of the time points assessed. Data analyzed using PERMANOVA.

(K) Heatmap of rhythmic genes in CV mice that lost rhythmicity in either GF or ABX mice.

(L) Venn diagrams and targeted enrichment for genes with lost rhythmicity. Rhythmicity analysis was conducted by linear modeling to a Fourier-decomposed sine and cosine element for circadian rhythmicity followed by Tukey-adjusted post-hoc comparisons.

(M) Triplot of redundancy analysis conducted between genes that constitute the circadian rhythm pathway in Gene Ontology, microbial status, and corticosterone. Ellipses indicate 95% confidence interval. Detailed statistical analysis can be found in Table S1.

Please cite this article in press as: Tofani et al., Gut microbiota regulates stress responsivity via the circadian system, Cell Metabolism (2024), https://doi.org/10.1016/j.cmet.2024.10.003

transcripts,[33] and by comparing both GF and ABX gene expression with CV mice, we identified transcripts that lost rhythmicity (Figure 1G).

The SCN is the master circadian pacemaker that coordinates a wide range of circadian functions through a transcriptional-translational negative feedback loop of core clock genes and proteins that lasts approximately 24 h (e.g., *Bmal1*, *Clock*, *Per1/2*, and *Cry1/2*),[34] which include maintaining appropriate glucocorticoid diurnal rhythmicity.[10,14] By using RNA sequencing, we show for the first time that manipulations to the gut microbiota lead to alterations in the clock machinery in the SCN. GF mice displayed arrhythmic levels of *Bmal1* and *Clock*, whereas ABX mice had an arrhythmic expression of *Cry2* and reversed rhythm of *Bmal1*, shifting the peak from the dark to the light phase (Figure 1H). These data indicate that the microbiota modulates central circadian rhythmicity. Moreover, both GF and ABX mice displayed different rhythmic patterns in the transcriptome overall, characterized as a shift in acrophases of the transcripts (Figure 1I). Furthermore, principal component analysis (PCA) followed by PERMANOVA indicated an influence of the microbiota in three out of the four time points assessed (Figure 1J).

Next, we show that genes in the SCN of both GF and ABX mice lose diurnal rhythmicity compared with CV (Figure 1K). To determine the functionality of genes that had lost rhythmicity, targeted enrichment analysis was conducted using Gene Ontology (GO).[35] Alongside the disruption to the circadian clock, genes that lost rhythmicity in the SCN compose important pathways for circadian regulation. Negative regulation of circadian rhythm and entrainment of circadian clock by photoperiod were enriched in ABX and detection of light stimulus was enriched in both groups (Figure 1L). We then assessed whether dysregulation in transcripts related to circadian pathways could be underlying the changes in the diurnal rhythm of corticosterone. By filtering the transcriptome with the GO term "circadian rhythm" and subsequently performing a redundancy analysis, we show that the variation in circadian pathways is able to explain the changes in corticosterone and the microbial status (Figure 1M). In summary, we demonstrate that the microbiota displays diurnal rhythmicity and regulates diurnal secretion of corticosterone, which is linked to disruption in circadian pathways in the SCN. These results suggest that the gut microbiota can influence central circadian rhythmicity and the downstream signaling mechanisms that synchronizes peripheral tissues with the central clock.

Rhythmicity of stress pathways in the brain is affected by the microbiota

Because the limbic system is essential for stress responsivity,[36] we then assessed the changes in rhythmicity in the transcriptome of the hippocampus and amygdala. Here, we show that these two regions also display changes in the circadian clock. Microbial manipulations altered the rhythmicity of *Bmal1*, *Clock*, *Per2*, *Cry2*, and *Ror*α in the hippocampus and *Clock*, *Per2*, and *Cry2* in the amygdala (Figure S2). Additionally, similar to the SCN, the transcriptome of GF and ABX mice also showed alterations in the acrophase of the transcripts in both regions (Figures 2A and 2C). PCA followed by PERMANOVA in the hippocampus demonstrated that ABX mice had changes in all the time points assessed, whereas GF had alterations in the dark phase (ZT17 and ZT23) (Figure 2B). In the amygdala, the analysis also indicated changes in ABX mice in all time points, with the exception of ZT17, and GF mice displayed changes in the dark phase, consistent with the hippocampus (Figure 2D).

We then aimed to investigate the lost rhythmicity in these regions induced by microbial status. Here, we demonstrate that 1,524 transcripts in the hippocampus and 505 in the amygdala lost rhythmicity in either GF or ABX mice (Figures 2E and 2G). Targeted enrichment indicated that such transcripts had function related to the stress system in both regions, with response to immobilization stress and response to glucocorticoid being altered (Figures 2F and 2H). To better understand the disruption to the stress system in GF and ABX mice and how it could be connected to the altered rhythmicity in corticosterone, we applied a random forest machine learning approach.[37] We first filtered the transcriptome with the GO term "response to glucocorticoid" and showed that based in the alterations induced by microbial manipulations in this pathway, the model created is able to identify microbial status with 70% accuracy in the amygdala and 89% in the hippocampus (Figures 2I and 2K). Moreover, this analysis also allowed us to understand which genes are the most important to identify the phenotypes. In the hippocampus, *Gsk3a* was the most important feature (Figure 2J), this gene has been shown to mediate stress-induced neuroinflammation in the hippocampus, which is linked to susceptibility to depression-like behavior.[38] Similarly, in the amygdala, *Hmgb1* was identified as an important feature for the classification (Figure 2L), which has been reported to be altered following stress in this region[39] and be involved in stress-induced depression.[40] Together, these data demonstrate that gut microbial manipulations alter the rhythmicity of stress pathways in regions key for regulating the stress response.

Diurnal oscillations in the central glutamate metabolism are altered by microbial status

Next, we assessed the diurnal changes in the metabolome of GF and ABX mice in the hippocampus and amygdala. Similar to the transcriptome, the rhythmic profile of metabolites was also changed by microbial status (Figures 3A and 3B). We then used a multi-omics approach to investigate the association between the rhythmicity in the transcriptome and metabolome of the two regions based on the KEGG database[41] (Figure 3C). It is known that the depletion of the gut microbiota can alter daily patterns of metabolic pathways in the brain,[42] but how changes in oscillating transcripts and metabolites interact remains completely unexplored. Both ABX and GF animals display a loss of rhythmicity in the metabolome in the regions assessed compared with CV mice (Figures 3D and 3E). Enrichment of metabolites that correlated with oscillations in functionally relevant genes across the day was related to pathways important for glutamate metabolism in both the amygdala (Figure 3F) and hippocampus (Figure 3G). Glutamate, the most abundant neurotransmitter in the brain, is known to be affected by stress in both the hippocampus and amygdala and is important in maintaining appropriate stress responsivity.[43–46] Glutamate, glutathione, and glutamine in the amygdala and 2-oxoglutarate and cysteine in the hippocampus displayed correlations with functionally relevant transcripts (Figures S3A and S3B). The levels of glutamate and the other

Please cite this article in press as: Tofani et al., Gut microbiota regulates stress responsivity via the circadian system, Cell Metabolism (2024), https://doi.org/10.1016/j.cmet.2024.10.003

CellPress
OPEN ACCESS

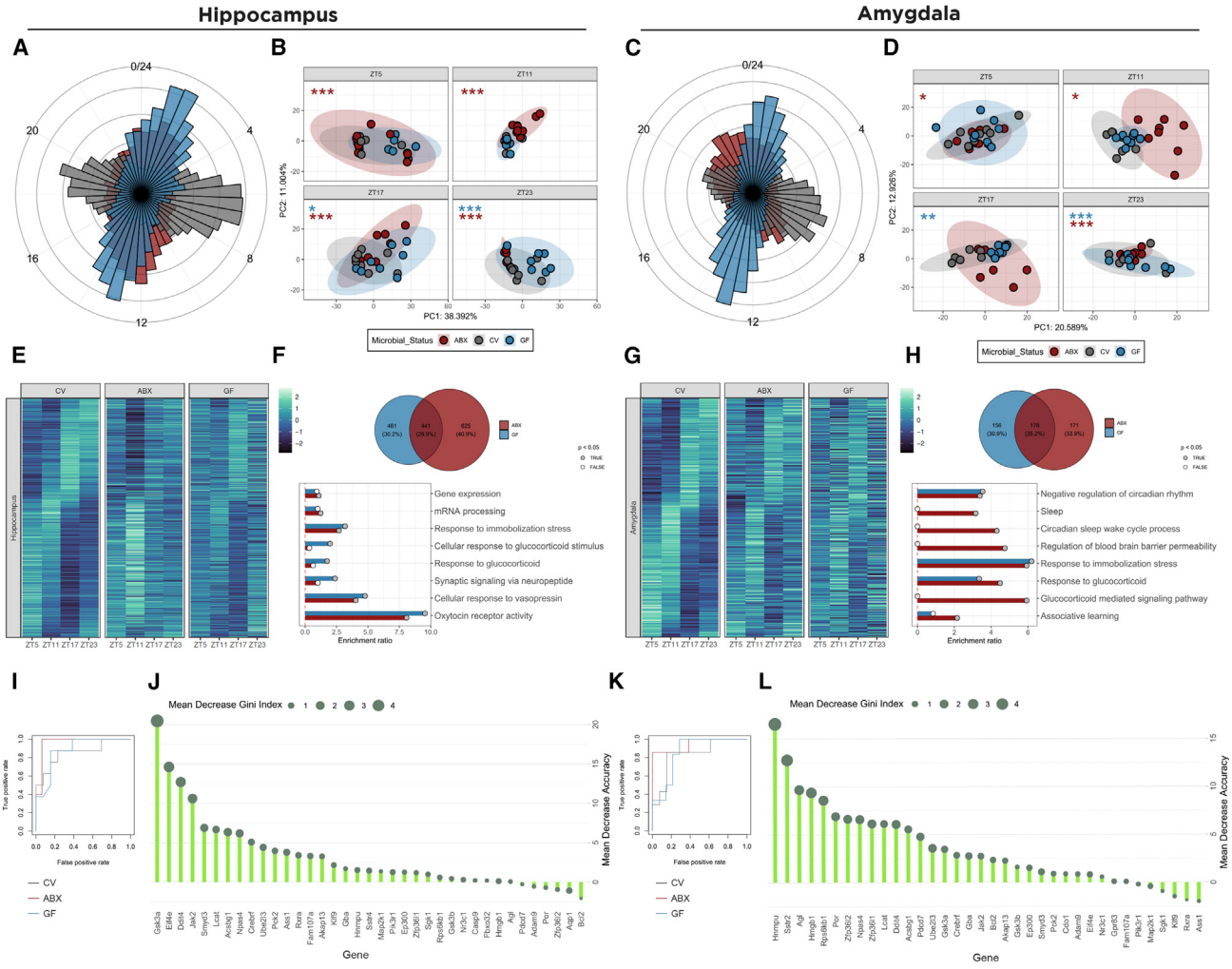

Figure 2. Absence of gut microbiota shapes the rhythmic oscillations of hippocampus and amygdala transcriptome

(A and C) Acrophase plots of all transcripts after rhythmicity analysis of (A) hippocampus (n = 6–8/group/time point) and (C) amygdala (n = 7–8/group/time point). Rhythmicity analysis was conducted by linear modeling to a Fourier-decomposed sine and cosine element for circadian rhythmicity followed by Tukey-adjusted post-hoc comparisons (bars represent the number of genes exhibiting their acrophase at each time point).

(B and D) Principal component analysis of the (B) hippocampus and (D) amygdala transcriptome in each of the time points assessed. Data analyzed using PERMANOVA.

(E and G) Heatmap of rhythmic genes in CV mice that lost rhythmicity in either GF or ABX mice in the (E) hippocampus and (G) amygdala.

(F and H) Venn diagrams and targeted enrichment for genes with lost rhythmicity in the (F) hippocampus and (H) amygdala. Rhythmicity analysis was conducted by linear modeling to a Fourier-decomposed sine and cosine element for circadian rhythmicity followed by Tukey-adjusted post-hoc comparisons.

(I and K) Receiver operating characteristic curve of random forest models showing the performance of the classification model in the (I) hippocampus and (K) amygdala.

(J and L) Importance plot for each of the variables used to generate the random forest model in the (J) hippocampus and (L) amygdala. Bars represent the mean decrease accuracy, an estimation of loss in predication power after that given variable is removed from the dataset, and circles represent mean decrease GINI, a measure of node impurity after that given variable is used to split the dataset. Detailed statistical analysis can be found in Table S1.

derived metabolites are changed across the day by disruption of the gut microbiota (Figures 3H and 3I). Through a joint-pathway analysis, we found that oscillations of metabolites and transcripts that compose the tripartite glutamate synapse are disrupted in both ABX and GF mice in both brain regions (Figures 3J, 3K, S3C, and S3D). Taken together, these data demonstrate that the transcriptomic changes induced by alterations in gut microbiota manifest in functional changes in brain glutamate metabolism across the day and could result in alterations in stress responsiveness.

Microbial depletion disrupts rhythmic patterns of the HPA axis

To dissect how the gut microbiota modulates diurnal rhythms in glucocorticoids, we then sought to understand what could be underlying the increase in the corticosterone peak in ABX mice (Figure 1F). Using gene expression assays, we investigated key genes of the circadian and stress systems across the three components of the HPA axis in ABX mice (Figure 4A): the PVN of the hypothalamus (Figures 4B and S4), pituitary (Figures 4C and S4), and adrenal gland (Figures 4D and S4). We observed

Please cite this article in press as: Tofani et al., Gut microbiota regulates stress responsivity via the circadian system, Cell Metabolism (2024), https://doi.org/10.1016/j.cmet.2024.10.003

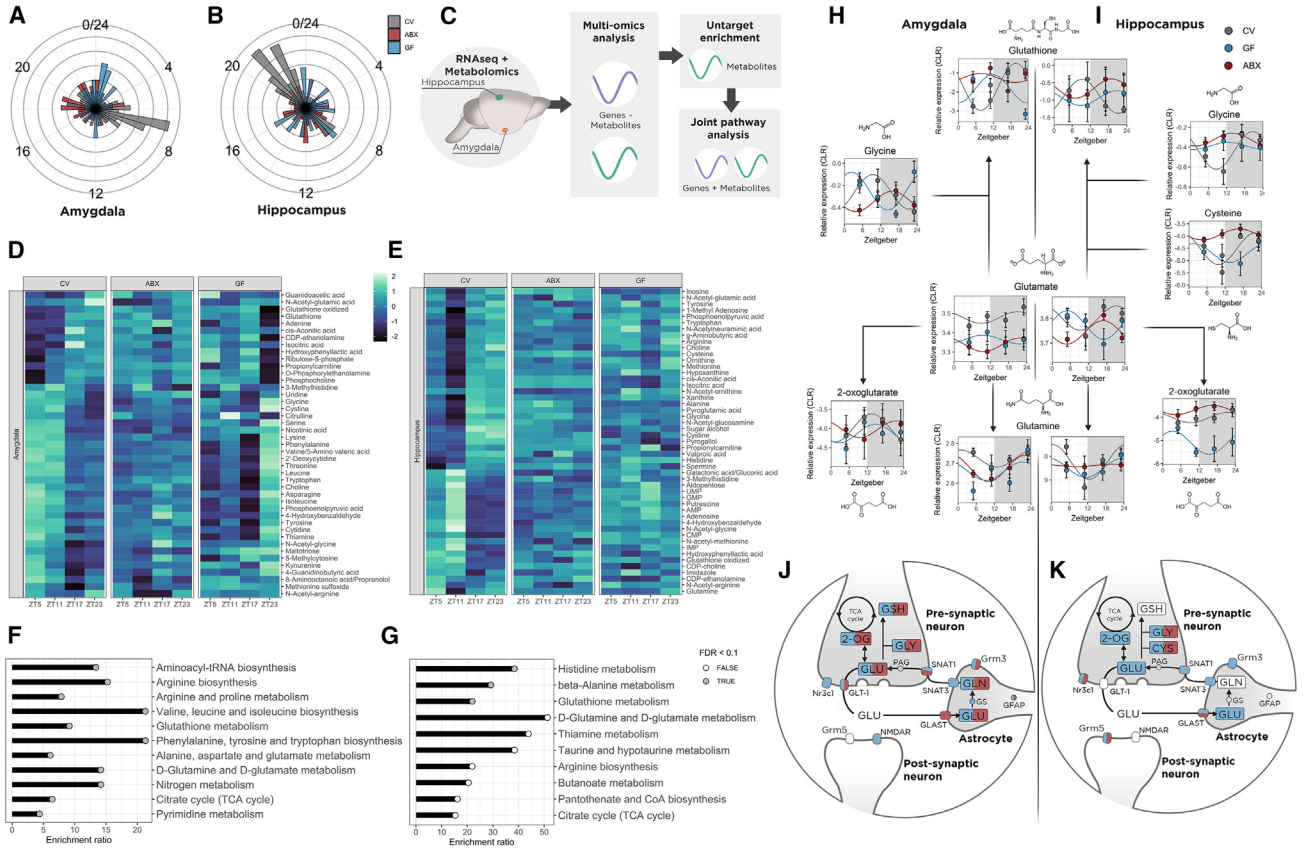

Figure 3. Disruption of gut microbiota leads to different diurnal patterns of glutamate metabolism in the brain

(A and B) Acrophase plot of oscillating metabolites in the (A) amygdala (n = 6–8/group/time point) and (B) hippocampus (n = 7–8/group/time point).

(C) Schematic of multi-omics analysis.

(D and E) Heatmaps of oscillating metabolites in (D) hippocampus and (E) amygdala. Metabolites were selected based on rhythmicity analysis in conventional animals ($p < 0.1$). Data displayed as group average. Rhythmicity analysis was conducted by linear modeling to a Fourier-decomposed sine and cosine element for circadian rhythmicity followed by Tukey-adjusted post-hoc comparisons.

(F and G) Untargeted enrichment of metabolites that correlated with functionally relevant genes in the RNA sequencing in (F) amygdala and (G) hippocampus.

(H and I) Representative pathway of glutamate metabolism in the (H) amygdala and (I) hippocampus. Line plots show the real (dot and error bar represent mean ± SEM) and predicted (line) metabolite expression for measured metabolites involved in glutamate metabolism. Rhythmicity analysis was conducted by linear modeling to a Fourier-decomposed sine and cosine element for circadian rhythmicity followed by Tukey-adjusted post-hoc comparisons.

(J and K) Schematic representing glutamate metabolism signaling in the tripartite synapse in (J) amygdala and (K) hippocampus, colors indicate transcripts/metabolites statistically altered in ABX (red) and GF (blue) mice. Detailed statistical analysis can be found in Table S1.

an increase in *Crh* and *Avp* at ZT11 (Figure 4B) in the PVN of ABX mice compared with vehicle-treated (VEH) controls with a similar ABX-induced increase in expression of *Pomc*, *Crhr1*, and *Crhr2* in the pituitary gland at the same time point (Figures 3C and S4Z). In the adrenal gland, no changes were observed in the expression of *Star*, but the rhythm of *Cyp21a*, an enzyme that catalyzes the hydrolyzation of steroid hormones, differed between ABX and VEH animals, and *Mcr2*, the receptor for adrenocorticotropic hormone (ACTH), was increased in ABX at ZT23 (Figure 4D). Glucocorticoid receptors (*Nr3c1*) interact with the circulating hormones and create a negative feedback that maintains appropriate HPA-axis function and stress responsiveness.[47] Here, we show that the rhythmicity of these receptors is disrupted in all three components of the HPA axis (Figures 4B–4D). Circadian gene expression in the PVN and in the adrenal gland is essential for maintaining diurnal rhythms of corticosterone.[5,48] PVN of ABX mice displays arrhythmic expression of *Per1* (Figure 4B), and disruption to the rhythmicity of core clock genes was observed in all three regions (Figures S5A–S5X). These data demonstrate that the gut microbiota modulates the rhythmic patterns of HPA-axis function, with ABX mice showing a hyper-activation at the circadian peak (ZT11). Because the majority of time-dependent changes were observed in the PVN and pituitary, the data also indicate that the altered peak of corticosterone in ABX mice may be driven in the brain.

Hypothalamic blood-brain barrier is impaired in microbially depleted animals

The blood-brain barrier is at the interface between the brain and circulating microbial signals.[49] This barrier is known for having circadian oscillations in function that can impact the stress response[50,51] and be altered upon chronic stress.[52] Given that microbial signals can modulate stress-induced corticosterone release[53] and genes that lost rhythmicity in the amygdala

Please cite this article in press as: Tofani et al., Gut microbiota regulates stress responsivity via the circadian system, Cell Metabolism (2024), https://doi.org/10.1016/j.cmet.2024.10.003

CellPress
OPEN ACCESS

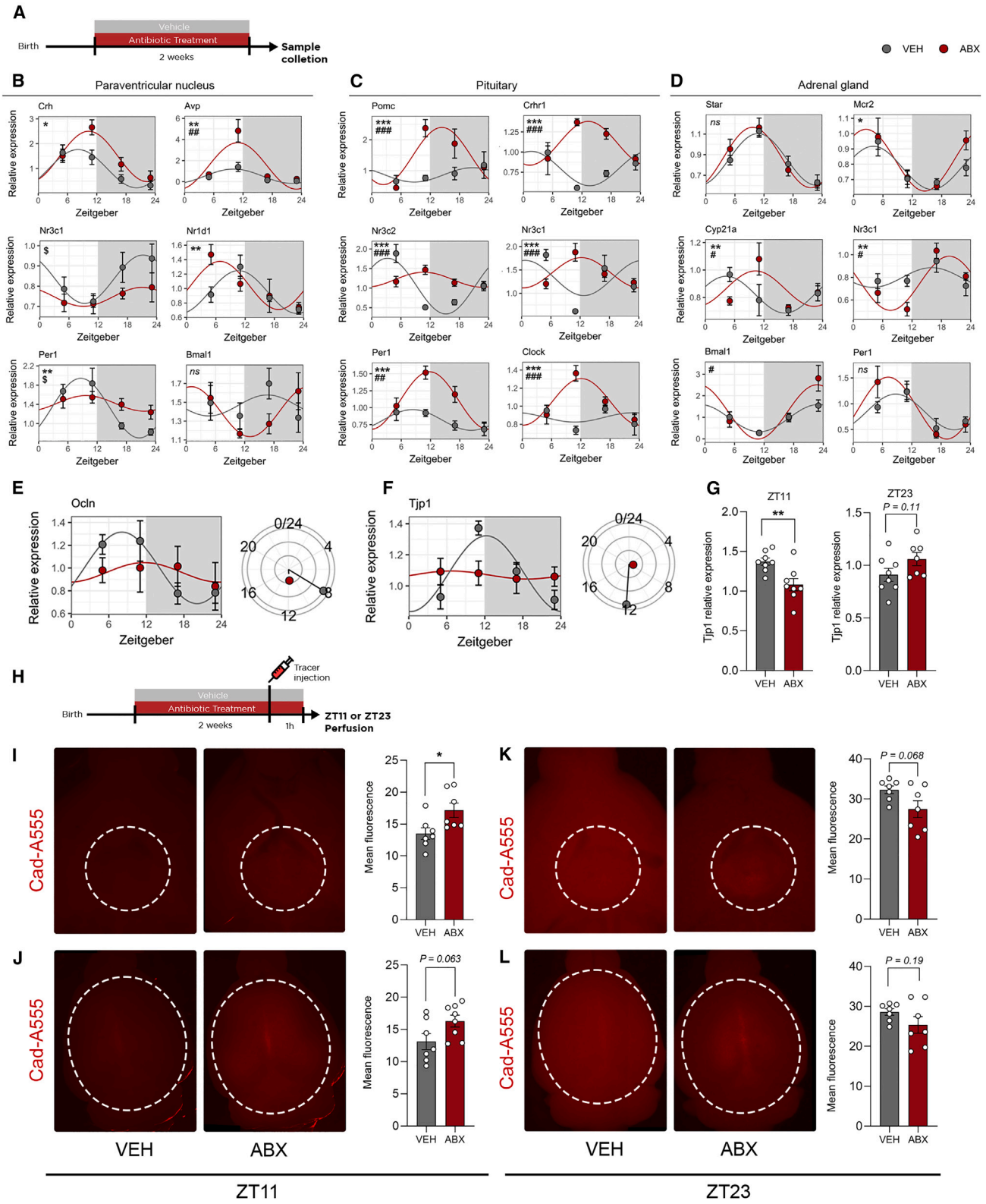

Figure 4. Microbial depletion alters diurnal rhythms of the HPA axis and disrupts the hypothalamic blood-brain barrier

(A) Experimental design schematic.

(B–D) Expression of genes related to stress and circadian systems in the PVN (B), pituitary (C), and adrenal gland (D) (n = 4–9/group/time point). Line plot shows the real (dot) and predicted (line) gene expression. Rhythmicity analysis was conducted by linear modeling to a Fourier-decomposed sine and cosine element for

(legend continued on next page)

Please cite this article in press as: Tofani et al., Gut microbiota regulates stress responsivity via the circadian system, Cell Metabolism (2024), https://doi.org/10.1016/j.cmet.2024.10.003

of ABX mice were related to the regulation of blood-brain barrier permeability (Figure 2), it was intriguing to test whether blood-brain barrier integrity was affected by microbial depletion at across the day. Indeed, the PVN of ABX mice displayed arrhythmic expression of tight junction proteins *Ocln* and *Tjp1* (Figures 4E and 4F). Additionally, *Tjp1* was reduced at ZT11 in ABX mice, whereas there was a trend for increased expression at ZT23 (Figure 4G). To determine if this altered gene expression translated to altered blood-brain barrier function, we conducted an *in vivo* permeability assay (Figure 4H). Here, we demonstrate that at ZT11 (when the *Tjp1* expression reaches its peak in VEH mice and ABX mice show no change from baseline), we observe an increase in permeability in the hypothalamus of ABX mice (Figure 4I). In addition, there was a trend for increased permeability in the cortex (Figure 4J). In contrast, at ZT23, where we observed an increase in the expression of *Tjp1* in ABX mice, we demonstrated a strong trend for a decrease in blood-brain barrier permeability in the hypothalamus and cortex (Figures 4K and 4L). These data indicate that, at the same time a hyper-activation of the HPA axis is observed, the PVN blood-brain barrier is more permeable to microbial signals in a time-of-day-dependent manner, which together could result in altered stress responsivity.

Regulation of the stress response by the gut microbiota is time-of-day dependent

This led to the hypothesis that microbiota-dependent alterations in rhythmic oscillations in the brain and circulating corticosterone could translate to changes in physiology and behavior in the context of stress. To better understand the impact of the ABX-induced exaggerated peak in glucocorticoid rhythm to stress responsivity, we performed acute restraint stress as pathways encoding for immobilization stress were altered in both hippocampus and amygdala (Figure 2). Mice were restrained for 15 min at either the ZT11 (peak) and ZT23 (trough), and plasma was collected following a tail snip for investigation of corticosterone stress response (Figure 5A). Although no difference induced by treatment was found within the non-stress condition, ABX mice stressed at ZT11, unlike VEH mice, show no increase in plasma corticosterone immediately following stress compared with their naive counterparts, whereas at ZT23, both groups show a strong stress response (Figures 5B and 5C).

Microbial depletion alters the behavioral response to stress

Next, we sought to assess whether these time-of-day effects in stress-induced corticosterone would impact stress-sensitive behaviors. Because social and anxiety-like behavior are modulated by both the microbiota and the stress system,[54,55] we performed open field test following acute restraint stress at ZT11, and reciprocal social interaction test at ZT11 and ZT23 (Figure 5D). Our results show that at ZT11, where the impairments in rhythmic HPA-axis function are concentrated, stressed VEH mice display a reduced total time of social interactions compared with their naive counterparts, whereas ABX mice showed no stress effect (Figures 5E and 5G). Moreover, to confirm that the behavioral alterations are driven by diurnal differences in the stress system, we repeated the behavioral test at ZT23 and demonstrated that both VEH and ABX animals show an effect of stress (Figures 5F and 5G). Using supervised machine learning,[56] we dissected the effects of microbial depletion and stress on social and non-social behaviors. Nose-body interactions were the most prevalent type of behavior among those investigated and were reduced following stress in VEH mice but not in ABX at ZT11 (Figure 5H). Anogenital sniffing and nose-nose interactions were also reduced in the stress VEH group compared with naive, although it was not statistically significant (Figures 5I and 5J). The sensitivity of different types of social interaction to acute stress was further established because we showed that nose-body interaction displayed an effect of stress in both ABX and VEH at ZT23, whereas the other types of interactions were unaffected (Figures 5K–5L). Non-social behaviors, rearing and grooming, were not altered by treatment, indicating that the changes driven by microbial depletion are restricted to social behaviors (Figures S5C and S5D). The open field test revealed an enhanced anxiety-like behavior in ABX mice, suggesting that alterations to the stress response at ZT11 will vary depending on the behavioral task and outcome measure (Figures S5D and S5E). To identify if such behavioral alterations are driven in the brain, we assessed the expression of genes important for HPA-axis function and social behavior regulation in the PVN 1 h after the reciprocal social interaction test (Figure S5G). Here, we show that, while stressed, VEH mice show increased *Fos* expression relative to both their naive counterparts and stressed ABX animals (Figure 5M), indicating a different neuronal activity in this region in response to stress in animals with a depleted microbiota. Moreover, *Avp* was also increased in stressed VEH animals (Figure 5O); because *Avp* is critical in regulating social behavior,[57] this further indicates a disruption of stress-responding regions in ABX mice.

Lastly, to confirm that these stress-induced alterations in social behaviors result from time-of-day-specific impairment of corticosterone release upon stress, we administered a corticosterone synthesis blocker, metyrapone, to VEH mice 40 min to 1 h prior to behavioral testing (Figure 5P). First, we confirmed that metyrapone administration prevented the stress-induced corticosterone release (Figure 5Q). The behavioral data indicated that by blocking the synthesis of corticosterone prior to stress exposure, the stress-induced social impairments can be prevented (Figure 5R). Additionally, we recapitulated our previous

circadian rhythmicity followed by Tukey-adjusted post-hoc comparisons. Statistics are reported as follows: * represents within time point differences, # represents pairwise rhythm differences, and $ represents loss of rhythmicity.
(E and F) Expression of (E) *Ocln* and (F) *Tjp1* across the day in the PVN (n = 4–9/group/time point).
(G) Expression of Tjp1 at ZT11 and ZT23 (n = 7–8/group/time point). Data analyzed using one-way ANOVA.
(H) Experimental design schematic.
(I and J) *In vivo* blood-brain barrier assessment of permeability at ZT11 (I) of the hypothalamus and (J) cortex (n = 7–8/group).
(K and L) *In vivo* blood-brain barrier assessment of permeability at ZT23 (K) of the hypothalamus and (L) cortex (n = 7/group). Data analyzed using unpaired t test.
Data expressed as mean ± SEM unless otherwise stated. */#$p < 0.05$, **/##$p < 0.01$, ***/###$p < 0.001$. Detailed statistical analysis can be found in Table S1.

Please cite this article in press as: Tofani et al., Gut microbiota regulates stress responsivity via the circadian system, Cell Metabolism (2024), https://doi.org/10.1016/j.cmet.2024.10.003

CellPress
OPEN ACCESS

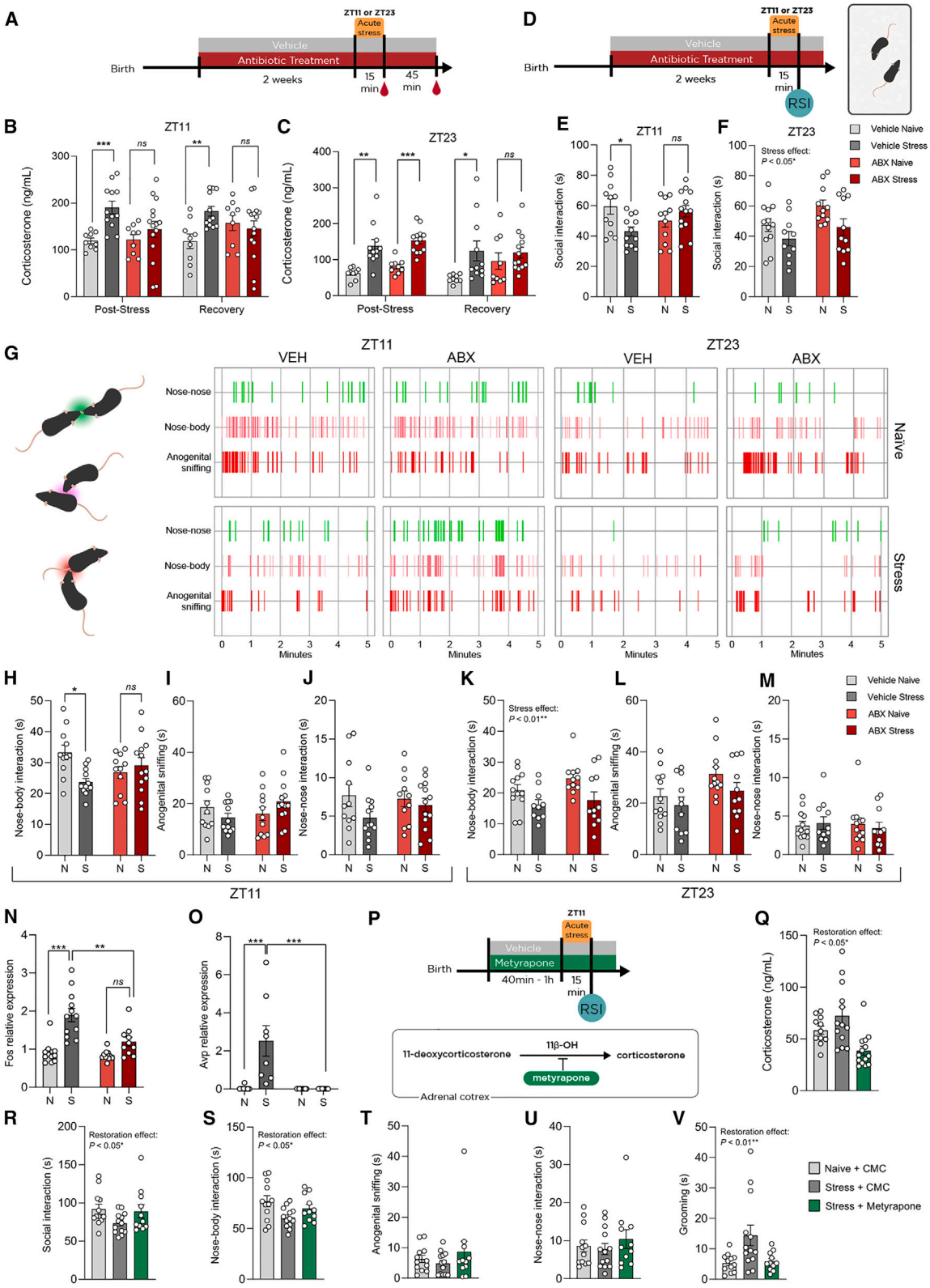

Figure 5. Microbial depletion leads to time-of-day effects on the stress response and stress-sensitive behaviors

(A) Experimental design schematic. (B and C) Corticosterone levels after acute stress (15 min) and after recovery (45 min) at (B) ZT11 and (C) ZT23 (n = 9–15/group). Data analyzed using three-way mixed ANOVA followed by Tukey-corrected pairwise comparisons.

(legend continued on next page)

Please cite this article in press as: Tofani et al., Gut microbiota regulates stress responsivity via the circadian system, Cell Metabolism (2024), https://doi.org/10.1016/j.cmet.2024.10.003

findings by demonstrating that nose-body interaction was the only type of social behavior that was restored after metyrapone administration (Figures 5S–5U). Alterations in grooming behavior were also restored by metyrapone (Figure 5V), whereas no effect on rearing was observed (Figure S5H). Taken together, our data show that baseline alterations in the HPA-axis function translates to altered corticosterone stress response in a time-of-day-specific manner. Such alteration was characterized as blunted corticosterone release upon stress in ABX mice at ZT11, which, in turn, leads to impairments in stress-sensitive social behaviors.

Disruption of the microbiota regulates the peak of corticosterone

To determine if the changes observed in circulating glucocorticoids were due to the microbes lost or those remaining following ABX exposure, we assessed the rhythm of corticosterone in animals treated with vancomycin (VAN), which targets gram-negative bacteria and gentamicin (GEN), which targets gram-positive bacteria (Figure 6A). Here, we show that the depletion of these groups of bacteria alone were not sufficient to drive the same effects on the daily rhythm of corticosterone as observed with a full ABX cocktail (Figure 6B). Next, we treated mice with the other two components of the antibiotic cocktail: imipenem (IMP) and ampicillin (AMP) and observed that the elevation in corticosterone at ZT11 is only driven by the full cocktail (Figure 6C). Following the same pattern as corticosterone, plasma ACTH also displayed an increase in ABX mice at ZT11 (Figures 6D and S6B). Additionally, the peak of corticosterone in female mice also was shown to be elevated compared with control animals, indicating that this change is not sex dependent (Figure 6E). To verify if the elevation in corticosterone could be reversed, following the 2 weeks of antibiotic treatment, ABX mice had the antibiotic cocktail removed and were exposed to bedding from VEH mice and allowed to recover for 1 or 2 weeks (Figure 6F). The data showed that 1 week was sufficient to restore normal corticosterone at ZT11 (Figure 6G).

It is established that the gut microbiota displays diurnal oscillations,[23] but how these oscillations change after antibiotic cocktail administration remains unexplored. To understand if these rhythmic diurnal changes in gut microbes are driving the alterations in HPA-axis function, we investigated the bacterial load in the caecum of ABX mice across the day and observed a distinct peak in bacterial load at ZT11 (Figure 6H). Lastly, we administered the same antibiotic cocktail to GF mice and measured plasma corticosterone at ZT11 (Figure 6I), and we confirmed that the increased peak observed is dependent on the disruption of the microbiota by antibiotics and not pharmacologically induced (Figure 6J). These results revealed that microbial depletion via antibiotics altered the rhythmic patterns of the gut bacterial load, leading to an aberrant peak of bacterial DNA. Together, such results indicate that this timed alteration to the gut microbiota is associated with the time-of-day-specific increase in plasma corticosterone.

Diurnal oscillations of gut microbes underlie changes in corticosterone release

To further establish causality, we then performed fecal microbiota transfer (FMT) collected at ZT11 and ZT23 from ABX mice at the end of the antibiotic treatment into GF animals (Figure 6K). This would confirm if transferring the peak of microbes observed in ABX mice would translate to higher corticosterone in recipient mice. The data indicated that the peak of corticosterone in the animals that received the FMT collected at ZT11 was elevated compared with animals that received FMT collected at ZT23 (Figure 6L). Gene expression assays indicated an increase of *Pomc* expression in the pituitary (Figure 6M) and reduced *Oxt* in the PVN (Figure 6N) of mice that received FMT from ABX mice collected at ZT11, further indicating that bacteria collected at different time of day from ABX mice can lead to different effects on the HPA axis. With the goal of confirming that diurnal oscillations of the gut microbiota impact corticosterone release, we repeated the experiment, but this time using the microbiota from VEH donors (Figure 6O). Here, we observed a trend toward increased corticosterone in animals that received the FMT collected at ZT11 compared with ZT23 (Figure 6P).

Finally, to uncover the microbial changes underlying the alterations in corticosterone, we performed metagenomic sequencing on cecal contents. At the genus level, we observed that the composition of the gut microbiota of mice that received FMT collected at ZT11 was different from that of those collected at ZT23 in animals receiving microbiota from both ABX and VEH mice (Figures 7A and 7B). Further analysis at the strain level indicated no changes in alpha-diversity metrics (Figures S7A and S7B), whereas beta-diversity analysis confirmed that the composition of the microbiota from recipient GF mice that received FMT from ABX or VEH animals was different depending on the time of day of collection (Figures 7C and 7D). Gut-brain[58] and gut-metabolic[59] modules analysis allowed us to interrogate some of the potential functional changes, which further indicated the effects of time of day on the microbiota. Within this analysis,

(D) Experimental design schematic.
(E) Total time of social interactions in the reciprocal social interaction test following acute stress at ZT11 (n = 11–12/group).
(F) Total time of social interactions in the reciprocal social interaction test following acute stress at ZT23 (n = 10–12/group). Data analyzed by two-way ANOVA followed by Tukey-adjusted post-hoc comparisons.
(G) Gantt chart of the occurrence of each of the assessed social behaviors.
(H–J) Duration of (H) nose-body interactions, anogenital (I) sniffing, and (J) nose-nose interactions at ZT11.
(K–M) Duration of (K) nose-body interactions, (L) anogenital sniffing, and nose-nose (M) interactions at ZT23.
(N and O) Expression of (N) *Fos* and (O) *Avp* in the PVN following reciprocal social interaction (n = 8–12/group).
(P) Experimental design schematic.
(Q) Corticosterone levels after the reciprocal social interaction test following acute stress at ZT11 with metyrapone administration.
(R) Total time of social interactions in the reciprocal social interaction test (n = 11–13/group).
(S–V) Duration of (S) nose-body interactions, (T) anogenital sniffing, (U) nose-nose interactions, and (V) grooming after metyrapone administration. Restoration effect was measured using planned orthogonal contrast. Data expressed as mean ± SEM unless otherwise stated. $^{*}p < 0.05$, $^{**}p < 0.01$, $^{***}p < 0.001$. Detailed statistical analysis can be found in Table S1.

Please cite this article in press as: Tofani et al., Gut microbiota regulates stress responsivity via the circadian system, Cell Metabolism (2024), https://doi.org/10.1016/j.cmet.2024.10.003

CellPress
OPEN ACCESS

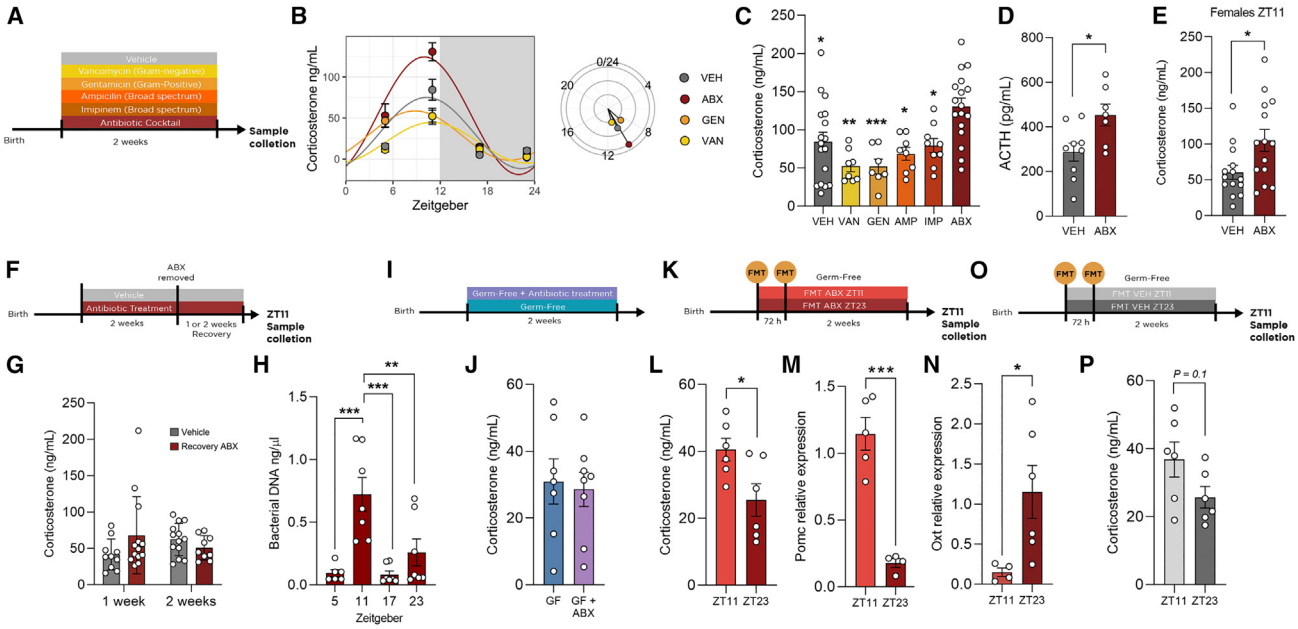

Figure 6. Microbes remaining after ABX exposure regulate the peak of glucocorticoid rhythm

(A) Experimental design schematic.

(B) Circulating plasma levels of corticosterone across the day with different antibiotic treatments (n = 6–17/group/time point). Line plot shows the real (dot and error bar represent mean ± SEM) and predicted (line) corticosterone levels. Rhythmicity analysis was conducted by linear modeling to a Fourier-decomposed sine and cosine element for circadian rhythmicity followed by Tukey-adjusted post-hoc comparisons.

(C) Plasma corticosterone at ZT11 in animals treated with different components of the antibiotic treatment. Data analyzed using one-way ANOVA followed by Tukey-adjusted post-hoc comparisons.

(D) Plasma levels of ACTH at ZT11 (n = 7–8/group). Data analyzed using one-way ANOVA.

(E) Corticosterone levels at ZT11 in female mice (n = 14/group). Data analyzed using unpaired t test.

(F) Experimental design schematic.

(G) Corticosterone levels following 1 or 2 weeks of recovery (n = 9–14/group/time point).

(H) Cecal bacterial DNA of ABX mice (n = 6–8/time point). Data analyzed using one-way ANOVA followed by Tukey-adjusted post-hoc comparisons.

(I) Experimental design schematic.

(J) Corticosterone levels at ZT11 of GF mice and GF mice treated with antibiotics (n = 7–8/group). Data analyzed using unpaired t test.

(K) Experimental design schematic.

(L) Corticosterone levels at ZT11 of GF mice that received FMT from ABX mice collected at ZT11 or ZT23 (n = 6/group).

(M and N) Expression of (M) *Pomc* in the pituitary and (N) *Oxt* in the PVN at ZT11 (n = 4–6/group).

(O) Experimental design schematic.

(P) Corticosterone levels at ZT11 of GF mice that received FMT from VEH mice collected at ZT11 and ZT23. Data analyzed using unpaired t test. Data expressed as mean ± SEM unless otherwise stated. *p < 0.05, ** p < 0.01, ***p < 0.001. Detailed statistical analysis can be found in Table S1.

we identified that 35.5% of the gut-brain modules and 59.5% of the gut-metabolic modules assessed were altered between FMT recipients of ZT11 and ZT23 of ABX donors (Figures S7C and S7D). No changes were observed in the recipient animals from VEH donors. The effects of time of day in the FMT collection was also observed at the strain level (Figures 7E and 7F). Although animal receiving FMT from both VEH and ABX animals displayed alterations in bacterial strains, such changes were more pronounced in ABX animals (Figures 7E and 7F). Although 5.9% of strains assessed in VEH-FMT receiving mice were different between ZT11 and ZT23 groups, 64.5% of strains were altered in mice that received FMT from ABX donors (Figure 7G). To further understand the interaction between corticosterone and the diurnal changes in gut microbiota, we performed a redundancy analysis and showed that the compositional changes in the microbiota are able to explain the variation in corticosterone in mice that received FMT from ABX but not in the groups that received from VEH mice (Figure 7H), what could be a result of more subtle alterations in the latter group. These results demonstrate that the microbial composition of GF mice that received FMT from ABX is different depending on the time of day of collection, which underlies the changes in circulating glucocorticoid.

Next, we leveraged the FMT microbiota datasets from ABX and VEH animals; by cross referencing, it allows us to identify convergent bacterial strains that could be altered in both experiments. Intriguingly, we showed that *L. reuteri* is the only strain altered when comparing ZT11 and ZT23 in both ABX and VEH-FMT recipients (Figure 7I). *L. reuteri* displayed an increase in ZT11 compared with ZT23 in both experiments (Figure 7J). To further confirm that this bacterial species could be underlying the microbial modulation of corticosterone, we assessed the diurnal rhythms of *L. reuteri* in both VEH and ABX animals. The relative abundance of *L. reuteri* in the mouse gut is rhythmic, reaching a peak in the light phase (Figure 7K). Moreover this microbe also composes the top 10 bacterial strains with

Please cite this article in press as: Tofani et al., Gut microbiota regulates stress responsivity via the circadian system, Cell Metabolism (2024), https://doi.org/10.1016/j.cmet.2024.10.003

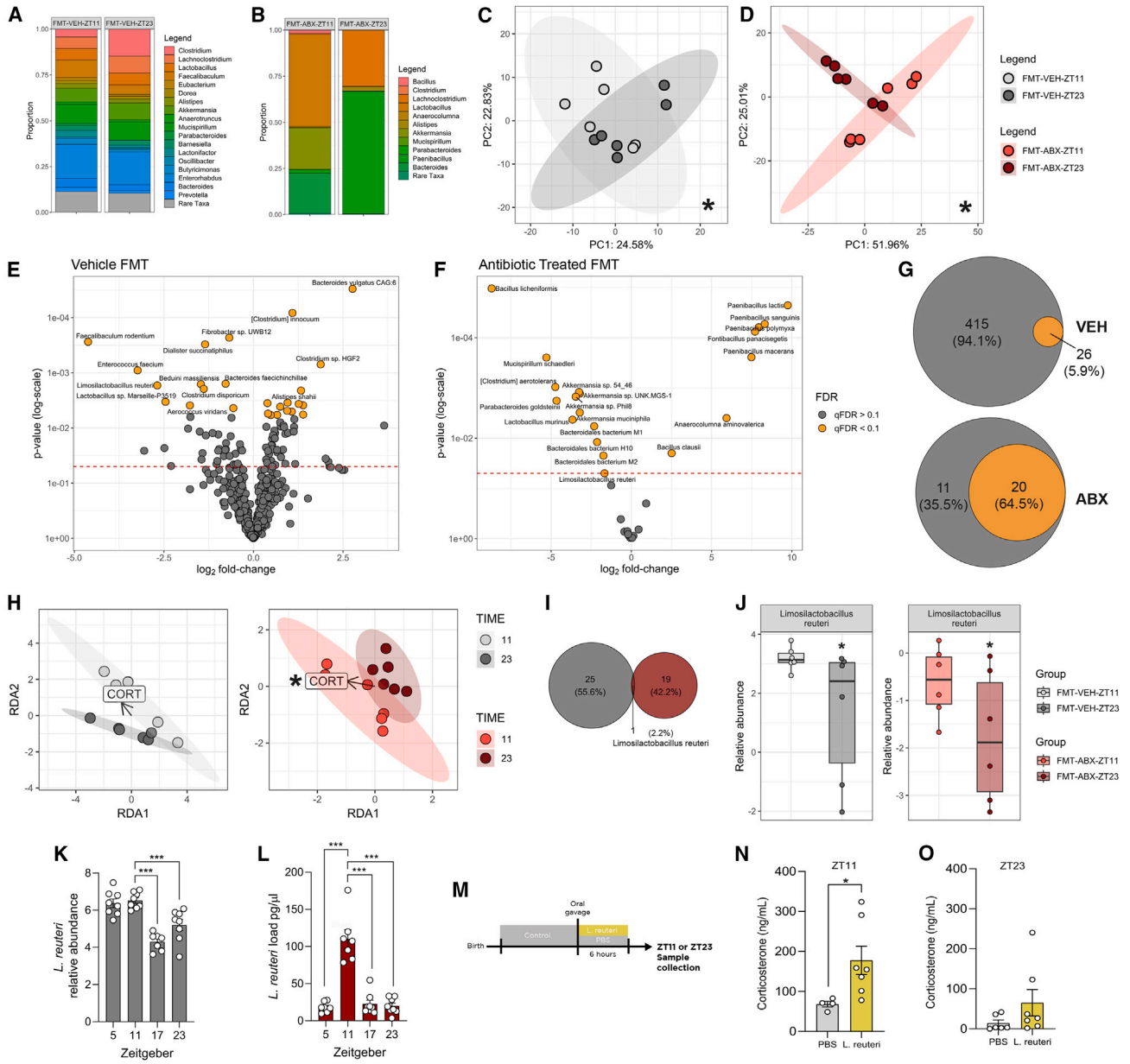

Figure 7. Alterations in microbial composition underlie changes in circulating corticosterone

(A–D) Bar plot comparing genus composing the microbiota of FMT recipients from VEH (A) and ABX (B) donors. Data presented as group average. Principal component analysis of microbial composition of cecal contents of FMT receivers from VEH (C) and ABX (D) donors in terms of β-diversity as measured in Aitchison distance. Ellipses indicate 95% confidence interval.

(E and F) Data analyzed with PERMANOVA. Volcano plot of (E) VEH and (F) ABX donors displaying the altered microbial strains by time-of-day in the caecum of FMT recipients. Data analyzed using one-way ANOVA.

(G) Venn diagram displaying the percentage of bacterial taxa altered in FMT recipient comparing ZT11 and ZT23 donors from VEH and ABX mice.

(H) Triplot of redundancy analysis conducted between microbial composition and corticosterone in recipients of FMT from VEH and ABX donors. Ellipses indicate 95% confidence interval.

(I) Venn diagram displaying the intersection between bacterial taxa that are altered between ZT11 and ZT23 in FMT recipients from VEH and ABX.

(J) *Limosilactobacillus reuteri* relative abundance in FMT recipients ($n = 6$ per group).

(K) Relative abundance of *L. reuteri* in the caecum of VEH mice across the day ($n = 6–8$ per group).

(L) Quantification of *L. reuteri* in the caecum contents of ABX mice across the day ($n = 7–8$ per group). Data analyzed using one-way ANOVA.

(M) Experimental schematic.

(N and O) Corticosterone levels following oral gavage of *L. reuteri* collected at ZT11 (O) and ZT23 (P) ($n = 4–7$ per group). Data analyzed using unpaired t test. $^{*}p < 0.05$, $^{**}p < 0.01$, $^{***}p < 0.001$. Detailed statistical analysis can be found in Table S1.

the highest diurnal amplitude (Figure 1). Following microbial depletion, the peak of *L. reuteri* is shifted to the same time as the peak of corticosterone (Figure 7L), further indicating that a potential role for these bacteria to drive the alterations in circulating glucocorticoids observed in ABX mice. Moreover, previous work has shown the *L. reuteri* is able to directly affect the PVN through the vagus nerve, having modulatory effects on social behavior.[60,61] To confirm that *L. reuteri* modulates the diurnal oscillations in corticosterone, we gavaged a strain of *L. reuteri* and 6 h later collected plasma at ZT11 or ZT23 (Figure 7M). *L. reuteri* led to an increase in corticosterone at ZT11 but not at ZT23 (Figures 7N and 7O). The data presented here highlight the effects of oscillation of gut bacteria on the circulating levels of corticosterone, further indicating that *L. reuteri* can modulate corticosterone release in a time-of-day-specific manner.

DISCUSSION

In this work, we provide compelling evidence that gut microbiota modulation of stress responsiveness exhibits diurnal rhythmicity. From comprehensive bioinformatic analysis of transcriptomic and metabolomic data, we show that the diurnal oscillations of stress and circadian relevant pathways are disrupted by modulating the gut microbiota in the SCN, amygdala, and hippocampus, key brain regions involved in both central circadian regulation and the behavioral stress response. Moreover, as the SCN is necessary to maintain circadian oscillations in glucocorticoids,[10] we demonstrate that the dysregulation of circadian rhythms driven by the gut microbiota in this region is linked to alterations in the diurnal rhythm of circulating corticosterone. Moreover, these alterations in corticosterone in microbially depleted mice were coupled with alterations in rhythmic HPA-axis function that are associated with time-of-day effects on the stress response and social behavior and directly linked to changes in the gut microbiota composition.

The results presented here have numerous implications. This study identifies diurnal rhythmicity as a key component of the regulation of the stress response by the gut microbiota. Although the gut microbiota has been shown to modulate the circadian and stress systems independently,[19,20,23,62] this is the first evidence that they are integrated together in a coordinated manner. We highlight that the modulation of glucocorticoids is time of day dependent and explore the implications of such regulation in the context of stress. Because glucocorticoids exert functions that are important for other systems,[63,64] the evidence presented here can be key to further understanding microbe-host interactions in the context of immunity and metabolism.

Many stress-related disorders involve alterations in the circadian system,[27,65,66] and changes in cortisol rhythmicity are associated with poor physical and mental health.[67] Perturbations in the gut microbiota are also observed in the same conditions.[28,68] With the modern environment involving increasing circadian disruption and stressor exposure, we need a better understanding of how our responses to these environmental factors are shaped and, more importantly, how they can be targeted to improve health. The discovery that the microbiota can regulate the interactions between the stress and circadian systems paves the way to explore interventions that can target gut microbes to modulate circadian and stress-related manifestations at the same time. Moreover, our identification of *L. reuteri* as a potential candidate circadian-sensitive strain demonstrate the potential importance of time of day for future psychobiotic interventions for stress-related disorders.

Limitations of the study

Although this study provides valuable scientific advances, it still has limitations, with further work being necessary for answering questions that remain open. Future research will aim to uncover whether the alterations to the corticosterone rhythm can be recovered upon colonization in GF mice, which are the microbial signals responsible for the modulation of diurnal HPA-axis function, and how they reach the brain to drive the regulation in the circadian and stress systems and modulate stress-sensitive brain areas at the transcriptomic and metabolic level. Additional work will also be necessary to assess the translation value of this findings, by investigating the concepts presented here in human cohorts across different geographies, diets, and lifestyles.

RESOURCE AVAILABILITY

Lead contact

Further information and requests for resources and reagents should be directed to and will be fulfilled by the lead contact, Professor John F. Cryan at j.cryan@ucc.ie.

Materials availability

This study did not generate new unique reagents.

Data and code availability

- Metagenomics and transcriptomic data have been deposited at the European Nucleotide Archive and are publicly available as of the date of publication. Metabolomics data are deposited at the Metabolomics Workbench[75] and are publicly available as of the date of publication. Accession numbers are listed in the key resources table.
- All other data used to generate main figures are available in Data S1.
- All original code has been deposited at GitHub and is publicly available. The URL is listed in the key resources table.

ACKNOWLEDGMENTS

The authors would like to thank Ruben Garcia Cabrerizo, Friederike Uhlig, Adam S. Lannon, Joana Cruz-Pereira, Anna Ratsika, Cristina R. Cardona, Naomi Gavioli, Serena Boscaini, Brendan Sharvin, Caoimhe Lynch, Marta Brocka, Michael Collins, Maria R. Aburto, Jatin Napgal, Gerard Moloney, Patrick Fitzgerald, Colette Manley, Frances O'Brien, Laicee Kenny, and Ken O'Riordan for their technical assistance and Kivia B.S. Santos for reviewing the manuscript. The research was conducted in the APC Microbiome Ireland, which is funded by Science Foundation Ireland (SFI/12/RC/2273_P2). The research project was funded by the Saks Kavanaugh Foundation.

AUTHOR CONTRIBUTIONS

Conceptualization, G.S.S.T., S.-J.L., C.E.G., G.C., and J.F.C.; investigation, G.S.S.T., S.-J.L., C.E.G., T.F.S.B., L.W., and P.S.; visualization, G.S.S.T. and T.F.S.B.; funding acquisition, J.F.C.; supervision, J.F.C.; writing—original draft, G.S.S.T.; writing—review and editing, G.S.S.T., S.-J.L., C.E.G., T.F.S.B., G.C., and J.F.C.

DECLARATION OF INTERESTS

J.F.C. has been an invited speaker at conferences organized by Bromotech and Nestle and has received research funding from Nutricia, Dupont/IFF,

and Nestle. G.C. has received honoraria from Janssen, Probi, and Apsen as an invited speaker; is in receipt of research funding from Pharmavite, Fonterra, Reckitt, Nestle, Tate, and Lyle; and is a paid consultant for Yakult, Zentiva, and Heel Pharmaceuticals. This support neither influenced nor constrained the contents of this article.

STAR★METHODS

Detailed methods are provided in the online version of this paper and include the following:

- KEY RESOURCES TABLE
- EXPERIMENTAL MODEL AND SUBJECT DETAILS
  - Studies in Animals
- METHOD DETAILS
  - Depletion of gut microbiota by antibiotic treatment
  - Acute restraint stress
  - Fecal Microbiota Transfer
  - In vivo blood brain barrier assessment
  - Behavior testing
  - Tissue collection
  - RNA extraction
  - Quantitative RT-PCR
  - Plasma ELISAS
  - DNA extraction and bacterial DNA quantification
  - Limosilactobacillus reuteri culture and treatment
  - Shotgun sequencing library preparation
  - Taxonomic and functional analysis
  - RNA-sequencing
  - Metabolomics
  - Bioinformatics and statistical analysis

SUPPLEMENTAL INFORMATION

Supplemental information can be found online at https://doi.org/10.1016/j.cmet.2024.10.003.

Received: September 27, 2023
Revised: April 12, 2024
Accepted: October 2, 2024
Published: November 5, 2024

REFERENCES

1. Koch, C.E., Leinweber, B., Drengberg, B.C., Blaum, C., and Oster, H. (2017). Interaction between circadian rhythms and stress. Neurobiol. Stress *6*, 57–67. https://doi.org/10.1016/j.ynstr.2016.09.001.
2. Chrousos, G.P., and Gold, P.W. (1992). The concepts of stress and stress system disorders. Overview of physical and behavioral homeostasis. JAMA *267*, 1244–1252. https://doi.org/10.1001/jama.1992.03480090092034.
3. Rijo-Ferreira, F., and Takahashi, J.S. (2019). Genomics of circadian rhythms in health and disease. Genome Med. *11*, 82. https://doi.org/10.1186/s13073-019-0704-0.
4. Oster, H. (2020). The interplay between stress, circadian clocks, and energy metabolism. J. Endocrinol. *247*, R13–R25. https://doi.org/10.1530/JOE-20-0124.
5. Jones, J.R., Chaturvedi, S., Granados-Fuentes, D., and Herzog, E.D. (2021). Circadian neurons in the paraventricular nucleus entrain and sustain daily rhythms in glucocorticoids. Nat. Commun. *12*, 5763. https://doi.org/10.1038/s41467-021-25959-9.
6. Spencer, R.L., Chun, L.E., Hartsock, M.J., and Woodruff, E.R. (2018). Glucocorticoid hormones are both a major circadian signal and major stress signal: How this shared signal contributes to a dynamic relationship between the circadian and stress systems. Front. Neuroendocrinol. *49*, 52–71. https://doi.org/10.1016/j.yfrne.2017.12.005.
7. Charmandari, E., Tsigos, C., and Chrousos, G. (2005). Endocrinology of the stress response. Annu. Rev. Physiol. *67*, 259–284. https://doi.org/10.1146/annurev.physiol.67.040403.120816.
8. Pezük, P., Mohawk, J.A., Wang, L.A., and Menaker, M. (2012). Glucocorticoids as Entraining Signals for Peripheral Circadian Oscillators. Endocrinology *153*, 4775–4783. https://doi.org/10.1210/en.2012-1486.
9. Balsalobre, A., Brown, S.A., Marcacci, L., Tronche, F., Kellendonk, C., Reichardt, H.M., Schütz, G., and Schibler, U. (2000). Resetting of Circadian Time in Peripheral Tissues by Glucocorticoid Signaling. Science *289*, 2344–2347. https://doi.org/10.1126/science.289.5488.2344.
10. Moore, R.Y., and Eichler, V.B. (1972). Loss of a circadian adrenal corticosterone rhythm following suprachiasmatic lesions in the rat. Brain Res. *42*, 201–206. https://doi.org/10.1016/0006-8993(72)90054-6.
11. Dunn, J., Scheving, L., and Millet, P. (1972). Circadian variation in stress-evoked increases in plasma corticosterone. Am. J. Physiol. *223*, 402–406. https://doi.org/10.1152/ajplegacy.1972.223.2.402.
12. Gibbs, F.P. (1970). Circadian variation of ether-induced corticosterone secretion in the rat. Am. J. Physiol. *219*, 288–292. https://doi.org/10.1152/ajplegacy.1970.219.2.288.
13. Kant, G.J., Mougey, E.H., and Meyerhoff, J.L. (1986). Diurnal Variation in Neuroendocrine Response to Stress in Rats: Plasma ACTH, β-Endorphin, β-LPH, Corticosterone, Prolactin and Pituitary Cyclic AMP Responses. Neuroendocrinology *43*, 383–390. https://doi.org/10.1159/000124553.
14. Leliavski, A., Shostak, A., Husse, J., and Oster, H. (2014). Impaired glucocorticoid production and response to stress in Arntl-deficient male mice. Endocrinology *155*, 133–142. https://doi.org/10.1210/en.2013-1531.
15. Cryan, J.F., and Dinan, T.G. (2012). Mind-altering microorganisms: the impact of the gut microbiota on brain and behaviour. Nat. Rev. Neurosci. *13*, 701–712. https://doi.org/10.1038/nrn3346.
16. Gaulke, C.A., Arnold, H.K., Humphreys, I.R., Kembel, S.W., O'Dwyer, J.P., and Sharpton, T.J. (2018). Ecophylogenetics Clarifies the Evolutionary Association between Mammals and Their Gut Microbiota. mBio *9*, e01348-18. https://doi.org/10.1128/mBio.01348-18.
17. Sharvin, B.L., Aburto, M.R., and Cryan, J.F. (2023). Decoding the neurocircuitry of gut feelings: Region-specific microbiome-mediated brain alterations. Neurobiol. Dis. *179*, 106033. https://doi.org/10.1016/j.nbd.2023.106033.
18. Lyte, J.M., Gheorghe, C.E., Goodson, M.S., Kelley-Loughnane, N., Dinan, T.G., Cryan, J.F., and Clarke, G. (2020). Gut-brain axis serotonergic responses to acute stress exposure are microbiome-dependent. Neurogastroenterol. Motil. *32*, e13881. https://doi.org/10.1111/nmo.13881.
19. Sudo, N., Chida, Y., Aiba, Y., Sonoda, J., Oyama, N., Yu, X.-N., Kubo, C., and Koga, Y. (2004). Postnatal microbial colonization programs the hypothalamic-pituitary-adrenal system for stress response in mice. J. Physiol. *558*, 263–275. https://doi.org/10.1113/jphysiol.2004.063388.
20. Leone, V., Gibbons, S.M., Martinez, K., Hutchison, A.L., Huang, E.Y., Cham, C.M., Pierre, J.F., Heneghan, A.F., Nadimpalli, A., Hubert, N., et al. (2015). Effects of Diurnal Variation of Gut Microbes and High-Fat Feeding on Host Circadian Clock Function and Metabolism. Cell Host Microbe *17*, 681–689. https://doi.org/10.1016/j.chom.2015.03.006.
21. Risely, A., Wilhelm, K., Clutton-Brock, T., Manser, M.B., and Sommer, S. (2021). Diurnal oscillations in gut bacterial load and composition eclipse seasonal and lifetime dynamics in wild meerkats. Nat. Commun. *12*, 6017. https://doi.org/10.1038/s41467-021-26298-5.
22. Thaiss, C.A., Zeevi, D., Levy, M., Zilberman-Schapira, G., Suez, J., Tengeler, A.C., Abramson, L., Katz, M.N., Korem, T., Zmora, N., et al. (2014). Transkingdom Control of Microbiota Diurnal Oscillations Promotes Metabolic Homeostasis. Cell *159*, 514–529. https://doi.org/10.1016/j.cell.2014.09.048.

23. Thaiss, C.A., Levy, M., Korem, T., Dohnalová, L., Shapiro, H., Jaitin, D.A., David, E., Winter, D.R., Gury-BenAri, M., Tatirovsky, E., et al. (2016). Microbiota Diurnal Rhythmicity Programs Host Transcriptome Oscillations. Cell *167*, 1495–1510.e12. https://doi.org/10.1016/j.cell.2016.11.003.

24. Zarrinpar, A., Chaix, A., Yooseph, S., and Panda, S. (2014). Diet and Feeding Pattern Affect the Diurnal Dynamics of the Gut Microbiome. Cell Metab. *20*, 1006–1017. https://doi.org/10.1016/j.cmet.2014.11.008.

25. Gheorghe, C.E., Leigh, S.-J., Tofani, G.S.S., Bastiaanssen, T.F.S., Lyte, J.M., Gardellin, E., Govindan, A., Strain, C., Martinez-Herrero, S., Goodson, M.S., et al. (2024). The microbiota drives diurnal rhythms in tryptophan metabolism in the stressed gut. Cell Rep. *43*, 114079. https://doi.org/10.1016/j.celrep.2024.114079.

26. Mukherji, A., Kobiita, A., Ye, T., and Chambon, P. (2013). Homeostasis in Intestinal Epithelium Is Orchestrated by the Circadian Clock and Microbiota Cues Transduced by TLRs. Cell *153*, 812–827. https://doi.org/10.1016/j.cell.2013.04.020.

27. Landgraf, D., McCarthy, M.J., and Welsh, D.K. (2014). Circadian Clock and Stress Interactions in the Molecular Biology of Psychiatric Disorders. Curr. Psychiatry Rep. *16*, 483. https://doi.org/10.1007/s11920-014-0483-7.

28. Nikolova, V.L., Smith, M.R.B., Hall, L.J., Cleare, A.J., Stone, J.M., and Young, A.H. (2021). Perturbations in Gut Microbiota Composition in Psychiatric Disorders: A Review and Meta-analysis. JAMA Psychiatry *78*, 1343. https://doi.org/10.1001/jamapsychiatry.2021.2573.

29. Teichman, E.M., O'Riordan, K.J., Gahan, C.G.M., Dinan, T.G., and Cryan, J.F. (2020). When Rhythms Meet the Blues: Circadian Interactions with the Microbiota-Gut-Brain Axis. Cell Metab. *31*, 448–471. https://doi.org/10.1016/j.cmet.2020.02.008.

30. Crumeyrolle-Arias, M., Jaglin, M., Bruneau, A., Vancassel, S., Cardona, A., Daugé, V., Naudon, L., and Rabot, S. (2014). Absence of the gut microbiota enhances anxiety-like behavior and neuroendocrine response to acute stress in rats. Psychoneuroendocrinology *42*, 207–217. https://doi.org/10.1016/j.psyneuen.2014.01.014.

31. Neufeld, K.M., Kang, N., Bienenstock, J., and Foster, J.A. (2011). Reduced anxiety-like behavior and central neurochemical change in germ-free mice. Neurogastroenterol. Motil. *23*, 255. https://doi.org/10.1111/j.1365-2982.2010.01620.x.

32. Eiden, L.E. (2013). Neuropeptide–Catecholamine Interactions in Stress. In Advances in Pharmacology (Elsevier), pp. 399–404.

33. Bastiaanssen, T.F.S., Leigh, S.-J., Tofani, G.S.S., Gheorghe, C.E., Clarke, G., and Cryan, J.F. (2023). Kronos: A computational tool to facilitate biological rhythmicity analysis). Preprint at bioRxiv. https://doi.org/10.1101/2023.04.21.537503.

34. Takahashi, J.S. (2017). Transcriptional architecture of the mammalian circadian clock. Nat. Rev. Genet. *18*, 164–179. https://doi.org/10.1038/nrg.2016.150.

35. Ashburner, M., Ball, C.A., Blake, J.A., Botstein, D., Butler, H., Cherry, J.M., Davis, A.P., Dolinski, K., Dwight, S.S., Eppig, J.T., et al. (2000). Gene Ontology: tool for the unification of biology. Nat. Genet. *25*, 25–29. https://doi.org/10.1038/75556.

36. Godoy, L.D., Rossignoli, M.T., Delfino-Pereira, P., Garcia-Cairasco, N., and de Lima Umeoka, E.H. (2018). A Comprehensive Overview on Stress Neurobiology: Basic Concepts and Clinical Implications. Front. Behav. Neurosci. *12*, 127. https://doi.org/10.3389/fnbeh.2018.00127.

37. Breiman, L. (2001). Random Forests. Mach. Learn. *45*, 5–32. https://doi.org/10.1023/A:1010933404324.

38. Cheng, Y., Pardo, M., Armini, R.S., Martinez, A., Mouhsine, H., Zagury, J.-F., Jope, R.S., and Beurel, E. (2016). Stress-induced neuroinflammation is mediated by GSK3-dependent TLR4 signaling that promotes susceptibility to depression-like behavior. Brain Behav. Immun. *53*, 207–222. https://doi.org/10.1016/j.bbi.2015.12.012.

39. Frank, M.G., Annis, J.L., Watkins, L.R., and Maier, S.F. (2019). Glucocorticoids mediate stress induction of the alarmin HMGB1 and reduction of the microglia checkpoint receptor CD200R1 in limbic brain structures. Brain Behav. Immun. *80*, 678–687. https://doi.org/10.1016/j.bbi.2019.05.014.

40. Zhang, H., Ding, L., Shen, T., and Peng, D. (2019). HMGB1 involved in stress-induced depression and its neuroinflammatory priming role: a systematic review. Gen. Psychiatry *32*, e100084. https://doi.org/10.1136/gpsych-2019-100084.

41. Bastiaanssen, T.F.S., Quinn, T.P., and Cryan, J.F. (2023). Knowledge-based Integration of Multi-Omic Datasets with Anansi: Annotation-based Analysis of Specific Interactions. Preprint at arXiv. https://doi.org/10.48550/ARXIV.2305.10832.

42. Smith, J.G., Sato, T., Shimaji, K., Koronowski, K.B., Petrus, P., Cervantes, M., Kinouchi, K., Lutter, D., Dyar, K.A., and Sassone-Corsi, P. (2022). Antibiotic-induced microbiome depletion remodels daily metabolic cycles in the brain. Life Sci. *303*, 120601. https://doi.org/10.1016/j.lfs.2022.120601.

43. Popoli, M., Yan, Z., McEwen, B.S., and Sanacora, G. (2011). The stressed synapse: the impact of stress and glucocorticoids on glutamate transmission. Nat. Rev. Neurosci. *13*, 22–37. https://doi.org/10.1038/nrn3138.

44. Nasca, C., Zelli, D., Bigio, B., Piccinin, S., Scaccianoce, S., Nisticò, R., and McEwen, B.S. (2015). Stress dynamically regulates behavior and glutamatergic gene expression in hippocampus by opening a window of epigenetic plasticity. Proc. Natl. Acad. Sci. USA *112*, 14960–14965. https://doi.org/10.1073/pnas.1516016112.

45. Dygalo, N.N., Kalinina, T.S., and Shishkina, G.T. (2020). Stress-induced expression pattern of glutamate signaling genes associated with anhedonia. Stress *23*, 700–707. https://doi.org/10.1080/10253890.2020.1812574.

46. Kinlein, S.A., Wallace, N.K., Savenkova, M.I., and Karatsoreos, I.N. (2022). Chronic hypothalamic-pituitary-adrenal axis disruption alters glutamate homeostasis and neural responses to stress in male C57Bl6/N mice. Neurobiol. Stress *19*, 100466. https://doi.org/10.1016/j.ynstr.2022.100466.

47. Gjerstad, J.K., Lightman, S.L., and Spiga, F. (2018). Role of glucocorticoid negative feedback in the regulation of HPA axis pulsatility. Stress *21*, 403–416. https://doi.org/10.1080/10253890.2018.1470238.

48. Oster, H., Damerow, S., Kiessling, S., Jakubcakova, V., Abraham, D., Tian, J., Hoffmann, M.W., and Eichele, G. (2006). The circadian rhythm of glucocorticoids is regulated by a gating mechanism residing in the adrenal cortical clock. Cell Metab. *4*, 163–173. https://doi.org/10.1016/j.cmet.2006.07.002.

49. Aburto, M.R., and Cryan, J.F. (2024). Gastrointestinal and brain barriers: unlocking gates of communication across the microbiota–gut–brain axis. Nat. Rev. Gastroenterol. Hepatol. *21*, 222–247. https://doi.org/10.1038/s41575-023-00890-0.

50. Schurhoff, N., and Toborek, M. (2023). Circadian rhythms in the blood–brain barrier: impact on neurological disorders and stress responses. Mol. Brain *16*, 5. https://doi.org/10.1186/s13041-023-00997-0.

51. Zhang, S.L., Lahens, N.F., Yue, Z., Arnold, D.M., Pakstis, P.P., Schwarz, J.E., and Sehgal, A. (2021). A circadian clock regulates efflux by the blood-brain barrier in mice and human cells. Nat. Commun. *12*, 617. https://doi.org/10.1038/s41467-020-20795-9.

52. Menard, C., Pfau, M.L., Hodes, G.E., Kana, V., Wang, V.X., Bouchard, S., Takahashi, A., Flanigan, M.E., Aleyasin, H., LeClair, K.B., et al. (2017). Social stress induces neurovascular pathology promoting depression. Nat. Neurosci. *20*, 1752–1760. https://doi.org/10.1038/s41593-017-0010-3.

53. Van De Wouw, M., Boehme, M., Lyte, J.M., Wiley, N., Strain, C., O'Sullivan, O., Clarke, G., Stanton, C., Dinan, T.G., and Cryan, J.F. (2018). Short-chain fatty acids: microbial metabolites that alleviate stress-induced brain-gut axis alterations. J. Physiol. *596*, 4923–4944. https://doi.org/10.1113/JP276431.

54. Wu, W.-L., Adame, M.D., Liou, C.-W., Barlow, J.T., Lai, T.-T., Sharon, G., Schretter, C.E., Needham, B.D., Wang, M.I., Tang, W., et al. (2021). Microbiota regulate social behaviour via stress response neurons in the

brain. Nature *595*, 409–414. https://doi.org/10.1038/s41586-021-03669-y.

55. Chen, J.-J., Xie, J., Zeng, B.-H., Li, W.-W., Bai, S., Zhou, C., Chen, W., Wei, H., and Xie, P. (2019). Absence of gut microbiota affects lipid metabolism in the prefrontal cortex of mice. Neurol. Res. *41*, 1104–1112. https://doi.org/10.1080/01616412.2019.1675021.
56. Goodwin, N.L., Choong, J.J., Hwang, S., Pitts, K., Bloom, L., Islam, A., Zhang, Y.Y., Szelenyi, E.R., Tong, X., Newman, E.L., et al. (2024). Simple Behavioral Analysis (SimBA) as a platform for explainable machine learning in behavioral neuroscience. Nat. Neurosci. *27*, 1411–1424. https://doi.org/10.1038/s41593-024-01649-9.
57. Veenema, A.H., and Neumann, I.D. (2008). Central vasopressin and oxytocin release: regulation of complex social behaviours. In Progress in Brain Research (Elsevier), pp. 261–276.
58. Valles-Colomer, M., Falony, G., Darzi, Y., Tigchelaar, E.F., Wang, J., Tito, R.Y., Schiweck, C., Kurilshikov, A., Joossens, M., Wijmenga, C., et al. (2019). The neuroactive potential of the human gut microbiota in quality of life and depression. Nat. Microbiol. *4*, 623–632. https://doi.org/10.1038/s41564-018-0337-x.
59. Vieira-Silva, S., Falony, G., Darzi, Y., Lima-Mendez, G., Garcia Yunta, R., Okuda, S., Vandeputte, D., Valles-Colomer, M., Hildebrand, F., Chaffron, S., and Raes, J. (2016). Species–function relationships shape ecological properties of the human gut microbiome. Nat. Microbiol. *1*, 16088. https://doi.org/10.1038/nmicrobiol.2016.88.
60. Buffington, S.A., Di Prisco, G.V., Auchtung, T.A., Ajami, N.J., Petrosino, J.F., and Costa-Mattioli, M. (2016). Microbial Reconstitution Reverses Maternal Diet-Induced Social and Synaptic Deficits in Offspring. Cell *165*, 1762–1775. https://doi.org/10.1016/j.cell.2016.06.001.
61. Sgritta, M., Dooling, S.W., Buffington, S.A., Momin, E.N., Francis, M.B., Britton, R.A., and Costa-Mattioli, M. (2019). Mechanisms Underlying Microbial-Mediated Changes in Social Behavior in Mouse Models of Autism Spectrum Disorder. Neuron *101*, 246–259.e6. https://doi.org/10.1016/j.neuron.2018.11.018.
62. Foster, J.A., Rinaman, L., and Cryan, J.F. (2017). Stress & the gut-brain axis: Regulation by the microbiome. Neurobiol. Stress *7*, 124–136. https://doi.org/10.1016/j.ynstr.2017.03.001.
63. Cain, D.W., and Cidlowski, J.A. (2017). Immune regulation by glucocorticoids. Nat. Rev. Immunol. *17*, 233–247. https://doi.org/10.1038/nri.2017.1.
64. Vegiopoulos, A., and Herzig, S. (2007). Glucocorticoids, metabolism and metabolic diseases. Mol. Cell. Endocrinol. *275*, 43–61. https://doi.org/10.1016/j.mce.2007.05.015.
65. Agorastos, A., Nicolaides, N.C., Bozikas, V.P., Chrousos, G.P., and Pervanidou, P. (2020). Multilevel Interactions of Stress and Circadian System: Implications for Traumatic Stress. Front. Psychiatry *10*, 1003. https://doi.org/10.3389/fpsyt.2019.01003.
66. Walker, W.H., Walton, J.C., DeVries, A.C., and Nelson, R.J. (2020). Circadian rhythm disruption and mental health. Transl. Psychiatry *10*, 28. https://doi.org/10.1038/s41398-020-0694-0.
67. Adam, E.K., Quinn, M.E., Tavernier, R., McQuillan, M.T., Dahlke, K.A., and Gilbert, K.E. (2017). Diurnal cortisol slopes and mental and physical health outcomes: A systematic review and meta-analysis. Psychoneuroendocrinology *83*, 25–41. https://doi.org/10.1016/j.psyneuen.2017.05.018.
68. Góralczyk-Bińkowska, A., Szmajda-Krygier, D., and Kozłowska, E. (2022). The Microbiota–Gut–Brain Axis in Psychiatric Disorders. IJMS *23*, 11245. https://doi.org/10.3390/ijms231911245.
69. Bastiaanssen, T.F.S., Quinn, T.P., and Loughman, A. (2023). Bugs as features (part 1): concepts and foundations for the compositional data analysis of the microbiome–gut–brain axis. Nat. Mental Health *1*, 930–938. https://doi.org/10.1038/s44220-023-00148-3.
70. Zhu, Q., Huang, S., Gonzalez, A., McGrath, I., McDonald, D., Haiminen, N., Armstrong, G., Vázquez-Baeza, Y., Yu, J., Kuczynski, J., et al. (2022). Phylogeny-Aware Analysis of Metagenome Community Ecology Based on Matched Reference Genomes while Bypassing Taxonomy. mSystems *7*, e0016722. https://doi.org/10.1128/msystems.00167-22.
71. Hsieh, T.C., Ma, K.H., and Chao, A. (2016). iNEXT: an R package for rarefaction and extrapolation of species diversity (H ill numbers). Methods Ecol. Evol. *7*, 1451–1456. https://doi.org/10.1111/2041-210X.12613.
72. Dixon, P. (2003). VEGAN, a package of R functions for community ecology. J. Veg. Sci. *14*, 927–930. https://doi.org/10.1111/j.1654-1103.2003.tb02228.x.
73. Chong, J., Wishart, D.S., and Xia, J. (2019). Using MetaboAnalyst 4.0 for Comprehensive and Integrative Metabolomics Data Analysis. Curr. Protoc. Bioinformatics *68*, e86. https://doi.org/10.1002/cpbi.86.
74. Bray, N.L., Pimentel, H., Melsted, P., and Pachter, L. (2016). Near-optimal probabilistic RNA-seq quantification. Nat. Biotechnol. *34*, 525–527. https://doi.org/10.1038/nbt.3519.
75. Sud, M., Fahy, E., Cotter, D., Azam, K., Vadivelu, I., Burant, C., Edison, A., Fiehn, O., Higashi, R., Nair, K.S., et al. (2016). Metabolomics Workbench: An international repository for metabolomics data and metadata, metabolite standards, protocols, tutorials and training, and analysis tools. Nucleic Acids Res. *44*, D463–D470. https://doi.org/10.1093/nar/gkv1042.
76. Mathis, A., Mamidanna, P., Cury, K.M., Abe, T., Murthy, V.N., Mathis, M.W., and Bethge, M. (2018). DeepLabCut: markerless pose estimation of user-defined body parts with deep learning. Nat. Neurosci. *21*, 1281–1289. https://doi.org/10.1038/s41593-018-0209-y.
77. Nath, T., Mathis, A., Chen, A.C., Patel, A., Bethge, M., and Mathis, M.W. (2019). Using DeepLabCut for 3D markerless pose estimation across species and behaviors. Nat. Protoc. *14*, 2152–2176. https://doi.org/10.1038/s41596-019-0176-0.
78. Langmead, B., and Salzberg, S.L. (2012). Fast gapped-read alignment with Bowtie 2. Nat. Methods *9*, 357–359. https://doi.org/10.1038/nmeth.1923.
79. Zhu, Q., Mai, U., Pfeiffer, W., Janssen, S., Asnicar, F., Sanders, J.G., Belda-Ferre, P., Al-Ghalith, G.A., Kopylova, E., McDonald, D., et al. (2019). Phylogenomics of 10,575 genomes reveals evolutionary proximity between domains Bacteria and Archaea. Nat. Commun. *10*, 5477. https://doi.org/10.1038/s41467-019-13443-4.
80. Mouse; Genome; Sequencing Consortium (2002). Initial sequencing and comparative analysis of the mouse genome. Nature *420*, 520–562. https://doi.org/10.1038/nature01262.
81. Aitchison, J., Barceló-Vidal, C., Martín-Fernández, J.A., and Pawlowsky-Glahn, V. (2000). Logratio Analysis and Compositional Distance. Math. Geol. *32*, 271–275. https://doi.org/10.1023/A:1007529726302.
82. Lubbe, S., Filzmoser, P., and Templ, M. (2021). Comparison of zero replacement strategies for compositional data with large numbers of zeros. Chemom. Intell. Lab. Syst. *210*, 104248. https://doi.org/10.1016/j.chemolab.2021.104248.
83. Bourgon, R., Gentleman, R., and Huber, W. (2010). Independent filtering increases detection power for high-throughput experiments. Proc. Natl. Acad. Sci. USA *107*, 9546–9551. https://doi.org/10.1073/pnas.0914005107.
84. Sing, T., Sander, O., Beerenwinkel, N., and Lengauer, T. (2005). ROCR: visualizing classifier performance in R. Bioinformatics *21*, 3940–3941. https://doi.org/10.1093/bioinformatics/bti623.

Please cite this article in press as: Tofani et al., Gut microbiota regulates stress responsivity via the circadian system, Cell Metabolism (2024), https://doi.org/10.1016/j.cmet.2024.10.003

STAR★METHODS

KEY RESOURCES TABLE

REAGENT or RESOURCE	SOURCE	IDENTIFIER
Chemicals, peptides, and recombinant proteins		
Ampicillin Sodium Salt	Discovery Fine Chemicals	69-52-3
Gentamicin Sulfate	Discovery Fine Chemicals	1405-41-0
Vancomycin Hydrochloride	Discovery Fine Chemicals	1404-93-9
Imipenem Monohydrate	Discovery Fine Chemicals	74431-23-5
Alexa Fluor™ 555 Cadaverine	Thermo Fisher Scientific	A30677
TaqMan™ PreAmp Master Mix	Applied Biosystems	4391128
Maxima H Minus Reverse Transcriptase	Thermo Fisher Scientific	EP0751
TaqMan™ Universal PCR Master Mix	Applied Biosystems	4305719
Metyrapone	R&D	3292
PowerUp™ SYBR™ Green Master Mix for qPCR	Applied Biosystems	A25741
BD Difco™ Lactobacilli MRS Broth	Fisher Scientific	288130
Critical commercial assays		
High-capacity cDNA reverse transcription kit	Thermo Fisher Scientific	4368814
mirVana miRNA isolation kit	Thermo Fisher Scientific	AM1561
QIAamp Fast DNA Stool Mini Kit	Qiagen	51604
Nextera XT DNA Library Preparation kit	Illumina	FC-131-1096
Qubit dsDNA High Sensitivity Assay Kit	Thermo Fisher Scientific	Q33230
Qiagen RNeasy Plus Micro Kit	Qiagen	74034
Corticosterone ELISA kit	Enzo Life Sciences	ADI-901-097
Mouse/Rat ACTH ELISA Kit	Abcam	ab263880
Femto Bacterial DNA Quantification Kit	Zymo Research	E2006
Epinephrine/Norepinephrine ELISA Kit	Abnova	KA3768
Deposited data		
Metagenomics and trasncriptomics data	European Nucleotide Archive	PRJEB64471
Metagenomics	European Nucleotide Archive	PRJEB58865
Metabolomics	Metabolomics Workbench	PR002130
Experimental models: Organisms/strains		
Mouse C57BL/6J	Envigo	057
Mouse C57BL/6J – germ-free and germ-free controls	F1 generated on site from mice purchased from Taconic Biosciences	B6-M; B6-F
Oligonucleotides		
Available in Table S3		N/A
Software and algorithms		
Kronos	Bastiaanssen et al.[33]	https://github.com/thomazbastiaanssen/kronos
FastQC	Babraham Bioinformatic	https://www.bioinformatics.babraham.ac.uk/projects/fastqc/
Bowtie2	Langmead and Salzberg[78]	http://bowtie-bio.sourceforge.net/bowtie2/index.shtml
Woltka	Zhu et al.[70]	https://github.com/qiyunzhu/woltka/blob/master/doc/wolsop.sh
Gomixer	Valles-Colomer et al.[58]	http://www.raeslab.org/omixer/application/show?page=download

(*Continued on next page*)

Please cite this article in press as: Tofani et al., Gut microbiota regulates stress responsivity via the circadian system, Cell Metabolism (2024), https://doi.org/10.1016/j.cmet.2024.10.003

Continued

REAGENT or RESOURCE	SOURCE	IDENTIFIER
iNEXT	Hsieh et al.[71]	https://cran.r-project.org/web/packages/iNEXT/index.html
Tjazi	Bastiaanssen et al.[69]	https://github.com/thomazbastiaanssen/Tjazi
Rstatix	Kassambara	https://CRAN.R-project.org/package=rstatix
Vegan	Dixon[72]	https://cran.r-project.org/web/packages/vegan/index.html
random forest	Breiman[37]	https://cran.r-project.org/web/packages/randomForest/index.html
Anansi	Bastiaanssen et al.[41]	https://github.com/thomazbastiaanssen/anansi
MetaboAnalyst	Chong et al.[73]	https://www.metaboanalyst.ca/home.xhtml
Kallisto	Bray et al.[74]	http://pachterlab.github.io/kallisto/
Other		
2018 Teklad global 18% protein rodent diet	Envigo	2018S
Zirconia/silica beads	BioSpec Products	11079125z
Nanodrop Spectrophotometer	Nanodrop Technologies	Nanodrop ND-1000
Tissue and Cell Homogenizer	MP Biomedicals	Model #6004-500

EXPERIMENTAL MODEL AND SUBJECT DETAILS

Studies in Animals

All experiments with animals were approved by the Animal Ethics Committee of University College Cork and Health Products Regulatory Authority (HPRA) under the project authorizations: AE19130/P047, AE19130/P160, and AE19130/P178 and carried out with accordance to the European Directive 2010/63/EU. Animals aged between 7 and 14 weeks were used during all experiments. For experiments using Germ-Free mice, C57/BL6 mice were acquired as breeding pairs from Taconic Biosciences, and subsequent generations were used. Germ-Free and conventional mice were maintained in cages with 2-4 animals under a 12-hour light/dark cycle with *ad libitum* autoclaved water and pelleted diet (Special Diet Services). Temperature was set to 21 ± 1°C and humidity to 55%-60%. Germ-free animals were housed in gnotobiotic isolators. Germ-free that received fecal microbiota transfer were housed in sterile individually ventilated cages (Tecniplast). For experiments not involving Germ-Free mice, male and female adult C57/BL6 mice were purchased from Envigo and grouped house in 2-4 per cage. Housing conditions were kept consistent with the other experiments.

METHOD DETAILS

Depletion of gut microbiota by antibiotic treatment

Mice received antibiotic treatment in *ad libitum* drinking water for a period of 14 days. The antibiotic cocktail consisted of ampicillin sodium salt (1g/L), gentamicin sulfate (1g/L), vancomycin hydrochloride (0.5g/L) and imipenem (0.25g/L) (Discovery Fine Chemicals). Water containing antibiotics was replaced every two days for the duration of the treatment and prepared freshly every time. Cages were randomly assigned to either vehicle or antibiotic treatment.

Acute restraint stress

The acute restraint stress protocol consisted of placing the mice inside a clean perforated polypropylene screw-cap 50mL conical tube for 15 minutes. Immediately before starting the stress, both stress and non-stress groups had approximately 0.5mm of the tip of their tail cut for repeated blood sampling using heparin-containing capillary tube and then transferred into a tube and kept on ice. Blood was collected a through tail snip before and after the stress and blood glucose was measured immediately after blood collection using Contour Next glucose meter (Bayer). After the stress, mice were returned to their respective cages and remained undisturbed for 45 minutes before having their blood sampled again. Blood was centrifuged for 5 min at 5000 g at 4°C, and plasma was collected and stored at −80°C for later analysis. In case of experiments exploring behavior following acute stress, blood was not collected. Mice that underwent behavioral testing did not undergo blood sampling. All experiments regarding stress were conducted in either Zeitgeber Time (ZT)11 or ZT23 (+/- 15 mins). Cages were randomly assigned to either naïve or stress groups.

Fecal Microbiota Transfer

Gut microbiota colonization of germ-free recipient mice (7-8 weeks) consisted of two inoculations of a 100μL fecal microbiota transfer (FMT) preparation 72 h apart. FMT preparation consisted of filtered murine cecal and colonic contents of antibiotic treated, or vehicle animals collected either at ZT11 or at ZT23. The contents were collected and immediately transferred into an anaerobic cabinet at

Please cite this article in press as: Tofani et al., Gut microbiota regulates stress responsivity via the circadian system, Cell Metabolism (2024), https://doi.org/10.1016/j.cmet.2024.10.003

37°C and subsequently diluted in sterile reduced phosphate-buffered saline (PBS). FMT preparations were stored in -80°C until the day of inoculation.

In vivo blood brain barrier assessment

Mice were induced and maintained under isoflurane anesthesia and then injected retro-orbitally with 100μl of Alexa Fluor 555-cadaverine fluorescent tracer (Thermo Fischer). The tracer was allowed to circulate for 1 hour. Animals were then intraperitoneally injected with pentobarbital (60-90 mg/kg) and perfused with 4% paraformaldehyde (PFA). Brains were post-fixated in 4% PFA for 4 hours and then transferred to a PBS + 0.02% Sodium Azide solution. Imaging was conducted the following day and fluorescence was quantified using ImageJ software and corrected against background per image.

Behavior testing

Reciprocal social interaction

Mice were placed in a clean arena (36cm x 20cm x 20cm) and allowed to acclimate for a period of 2 minutes, before another novel age and sex matched mouse is introduced to the cage. Interactions were then recorded for a period of 5 minutes. All test animals were socially isolated for 4 hours before testing started. Social behaviors were defined as anogenital sniffing, nose-body interaction and nose-nose interaction. Grooming and rearing were considered as nonsocial behaviors. Behavior analysis was conducted using Deeplabcut 2.3 for tracking pose estimation,[76,77] and complex social and nonsocial behaviors were scored using behavior classifiers in SimBA 1.5.[56] Mice were intraperitoneally injected with 50mg/kg metyrapone (R&D) to block synthesis of corticosterone. The drug was dissolved in 0.5% carboxymethylcelulose (Sigma). Reciprocal social interaction was conducted 40 min – 1 hour after injection.

Open field

Mice were placed in an empty squared arena (45cm x 45cm) illuminated to 60 lux and were recorded for 10 minutes using a celling camera. Locomotion and time in center were scored using deep-learning informed software as described above.

Tissue collection

Mice were transferred to a cull room and immediately decapitated. Trunk blood was collected into K2 EDTA lavander-top vacutainer (BD Life Sciences) and then centrifuged at 3500 g for 15 minutes at 4°C. Tissues were then harvested, stored in PCR-grade tubes and flash-frozen in dry ice. Samples were stored in -80°C until further analysis.

RNA extraction

RNA from pituitary, adrenal glands, hippocampus and amygdala was extracted using mirVana™ miRNA isolation kit (Thermo Fisher Scientific) according to the manufacturer's instructions using zirconia/silica beads (BioSpec) in a bead beater (MP Biomedical). RNA from the paraventricular nucleus (PVN) and suprachiasmatic nucleus (SCN) was extracted using RNAeasy Micro Plus kit (Qiagen) following manufacturer's instructions. RNA concentration and quality was then measured using Nanodrop Spectophtometer (Nanodrop technologies).

Quantitative RT-PCR

Extractions from the pituitary and adrenal glands were reverse transcribed using a HighCapacity cDNA Reverse Transcription kit (Thermo Fisher Scientific). RNA from the PVN was reversed transcribed with Maxima H Minus Reverse Transcriptase (Thermo Fisher Scientific) and preamplified using TaqMan™ PreAmp Master Mix (Applied Biosystems). TaqMan Gene Expression Master Mix (Applied Biosystems) was used in real-time PCR. Primers (Integrated DNA Technology) codes can be found on the key resources table. *Hprt* and *Actb* were used as housekeeping genes. The expression of targeted genes was normalized to the mean of the housekeeping genes. The further analysis of relative gene expression was done by the ΔΔCT method using an independent calibrator.

Plasma ELISAS

Plasma adrenaline and noradrenaline were quantified using the enzyme-linked immunosorbent assay (ELISA) kit (Abnova) following the manufacturer's instructions. The protocol was slighty modified where 15μL of plasma was used instead of 300μL. Plasma corticosterone (Enzo lifesciences) and ACTH (Abcam) were quantified using an ELISA kit, according to manufacturer's instructions. Absorbance was read using a Biotek Synergy H1 plate reader equiped with Gen5 software (Biotek).

DNA extraction and bacterial DNA quantification

DNA from caecal contents was extracted using the QIAmp Fast DNA Stool kit (Qiagen) according to the manufacturer's instructions using zirconia/silica beads (Biospec). After dilution, bacterial DNA load was assessed using Femto Bacterial DNA quantification kits according to the manufacturer's instructions (Zymo Research). Quantification of *L. reuteri* was performed using qPCR using PowerUp SYBR Green Master Mix (Applied Biosystems) according to manufacturer's protocol. Primers targeting the 16S ribosomal subunit of *L. reuteri* were used.

Limosilactobacillus reuteri culture and treatment

Limosilactobacillus reuteri strain MM4-1A was cultured in MRS broth (BD Difco, Fisher Scientific) supplemented with 0.5% L-cysteine hydrochloride ((w/v), Sigma-Aldrich) at 37°C in an anaerobic chamber (80% N_2, 10% CO_2, 10% H_2). Cultures were grown until the

Please cite this article in press as: Tofani et al., Gut microbiota regulates stress responsivity via the circadian system, Cell Metabolism (2024), https://doi.org/10.1016/j.cmet.2024.10.003

early stationary phase (~OD600 of 1.7). The bacterial cells were washed twice by centrifugation at 4000 rpm for 10 minutes and re-suspension in phosphate-buffered saline (PBS). After the second washing step, bacterial cell pellets were resuspended in PBS with 20% glycerol (v/v) and stored at −80°C until use. Purity of the inoculum was verified by Sanger sequencing of the 16S rRNA gene. Specifically, bacterial cell pellets were collected from liquid cultures for DNAextraction. Obtained DNA was used as a template for PCR targeting the 16S rRNA gene using universal bacterial primers (27F2: AGA GTT TGA TCA TGG CTC A, 1492r:TAC GGT TAC CTT GTT ACG ACT T). Obtained sequences were analysed in BioEdit 7.2 and identified in nucleotide-Basic Local Alignment Search Tool to identify closest match. The experimental groups received 100μl of live bacteria at a concentration of $3x10^{10}$ CFU/ml. Mice were sampled 6 hours after the oral gavage.

Shotgun sequencing library preparation

Whole genome sequencing sequencing library preparation used the Nextera XT DNA Library Preparation kit (Ilumina) and followed the Nextera XT DNA Library Preparation Guide. Samples of DNA were diluted to a concentration of 0.2 ng/μL and incubated at 55°C for 7 minutes. Next, Pair-ended Nextera indexes were added, and 12 cycles of amplification process were performed. Samples were then purified with AMPure XP beads (Beckman Coulter Life Sciences) according to the manufacturer's instructions. To assess molarity, DNA concentration was quantified using Qubit dsDNA High Sensitivity Assay (Thermofisher Scientific) and amplicon size was measured by Agilent Bioanalyser 2100. Finally, 1 mM were pooled before loading on the Illumina NextSeq plataform for 150 bp paired-end sequencing.

Taxonomic and functional analysis

Raw sequences underwent quality checks using the FastQC program with the default quality score of 30 threshold. Shotgun sequencing data were then cleaned of host genome sequences and were then filtered using Bowtie[78] via the Kneaddata wrapper program with the following parameters: ILLUMINACLIP:/NexteraPE-PE.fa:2:30:10, SLIDINGWINDOW:5:25, MINLEN:60, LEADING:3, TRAILING:3. Reads were aligned to the Web of Life database[79] using Bowtie2 and taxonomic and functional profiling of the microbial community was performed using woltka.[70] Next, the uniref90-based gene abundance matrix was further collapsed by KEGG Orthology (KO) term mapping via the "woltka tools collapse" function provided within woltka. Woltka SOP is available online (https://github.com/qiyunzhu/woltka/blob/master/doc/wolsop.sh). Gut-Brain Modules (GBMs)[58] and Gut-Metabolic Modules (GMMs)[59] were calculated using the R version of the Gomixer tool.

RNA-sequencing

mRNA sequencing was conducted by Azenta (Standard RNA-Seq for hippocampus and amygdala, and *ultra-low input* RNA-Seq for SCN) on the Illumina NovaSeq 6000 (S4 flow cell, 150bp paired-end lane yielding 2.5 billion read pairs). Reference genome of obtained sequences was performed using the reference annotation: Mus musculus (organism), GRCm38, UCSC, genome browser (GRCm38.p6), Ensemble.[80] Reads were assessed and filtered for quality using FastQC using default parameters. Genes were annotated and counted using kallisto[74] using default parameters.

Metabolomics

The hippocampus and amygdala metabolomics was conducted by MS-Omics as follows. The analysis was carried out using a Thermo Scientific Vanquish LC coupled to Thermo Q Exactive HF MS. An electrospray ionization interface was used as ionization source. Analysis was performed in negative and positive ionization mode. The UPLC was performed using a slightly modified version of the protocol described by Catalin et al. (UPLC/MS Monitoring of Water-Soluble Vitamin Bs in Cell Culture Media in Minutes, Water Application note 2011, 720004042en). Peak areas were extracted using Compound Discoverer 3.1 (Thermo Scientific). Identification of compounds were performed at four levels; Level 1: identification by retention times (compared against in-house authentic standards), accurate mass (with an accepted deviation of 3ppm), and MS/MS spectra, Level 2a: identification by retention times (compared against in-house authentic standards), accurate mass (with an accepted deviation of 3ppm). Level 2b: identification by accurate mass (with an accepted deviation of 3ppm), and MS/MS spectra, Level 3: identification by accurate mass alone (with an accepted deviation of 3ppm).

Bioinformatics and statistical analysis

Biostatistics were undertaken in R (version 4.2.2) with the Rstudio GUI (version 2022.07.2 build 576). All data are represented as mean ± SEM. Normality was assessed employing the Shapiro–Wilk test and for equality of variances using the Levene's test. Unpaired t-test was used to compare data between two groups. ANOVA with the appropriate explanatory factors was used to analyze tests with multiple groups and levels. In order to assess differences between singular pairs of groups we used Tukey-adjusted post-hoc comparisons. The restoration effect by metyrapone was analyzed by planned orthogonal contrast. Rhythmicity analysis was conducted by fitting linear models for each variable to a fourier-decomposed sine and cosine element as described previously.[33] Code used to fit these models can be found online at https://github.com/thomazbastiaanssen/kronos. Technical outliers were removed prior to statistical analyses and statistical outliers were identified using Grubb's test.

'Omics datasets

'Omics data analysis (metabolomics, transcriptomics and metagenomics) was performed on centred log-ratio ratio (CLR) transformed values.[81] Principal component analysis was performed on CLR-transformed values. Zeroes were replaced using the 'const'

approach described by Lubbe and colleagues.[82] The PERMANOVA implementation from the vegan library was used to find structural differences between microbial status on a compositional level. Rhythmicity analysis was conducted by fitting linear models for each CLR-transformed value. To find features that were differentially abundant based on microbial status within each timepoint, data was split and linear models fitted using the CLR-transformed values with microbial status as an explanatory variable. To correct for multiple testing involved in the study, features were selected based on the Benjamini-Hochberg procedure with a q-value of 0.1 as a threshold. This procedure controls the False Discovery Rate (FDR) using sequential modified Bonferroni correction for multiple testing. Custom R scripts and functions are available online at https://github.com/thomazbastiaanssen/Tjazi [69].

RNA sequencing analysis

RNA-seq data was filtered for transcripts with counts with a prevalence > 20% across samples and statistical testing was conducted after variance filtering using the genefilter library in R,[83] with 0.6 set as the cutoff. For enrichment analysis, we identified *a priori* in the Gene Ontology database[35] terms that are relevant for the scope and objectives of the study design and then assessed enrichment by using the base R stats phyper implementation of hypergeometric test. Rhythmicity and within timepoint analysis were conducted as described above. To understand if the alteration in gene encoding for circadian rhythms explained the variance in other variables, redundancy analysis (RDA) was conducted using R package vegan.[72] Random forest model was created using the R package randomForest and receiving operating characteristic curve (ROC) was calculated using R package ROCR.[84]

Multi-omics integration analysis

In order to assess associations between the transcriptomics and metabolomics all relevant transcripts were converted to KEGG orthologues and metabolites to KEGG compounds. Then we fitted linear mixed-effects models between those pairs of features that shared membership in a KEGG-pathway. This method, Anansi (Annotation based analysis of specific interactions), is described in detail here Bastiaanssen et al.[41] Custom R scripts and functions are available online at https://github.com/thomazbastiaanssen/anansi. Metabolites with a significant correlation ($q < 0.1$) were then used for enrichment analysis using the MetaboAnalyst online pipeline,[73] choosing the murine KEGG library as a reference. Rhythmicity and within timepoint analysis were conducted as described above.

Shotgun metagenomic analysis

Shotgun metagenomic data was filtered for taxa with counts with a prevalence > 20% across samples and statistical testing was conducted after variance filtering using the genefilter library in R,[83] with 0.5 set as the cutoff. Beta-diversity was computed in terms of Aitchison distance, or Euclidean distance between CLR-transformed data. Alpha-diversity was computed using the iNEXT library.[71] To understand if the compositional changes in the microbiota explained the variance in other variables, redundancy analysis (RDA) was conducted using R package vegan.[72] Differential abundance of microbial taxa, GBMs, and GMMse were determined using linear models as previous described.